NAS8-37136

March 1989

Appendix B
Liquid Rocket
Booster Acoustic
and Thermal
Environments
Remtech Report
RTN 186-02

Liquid Rocket Booster (LRB) for the Space Transportation System (STS) Systems Study

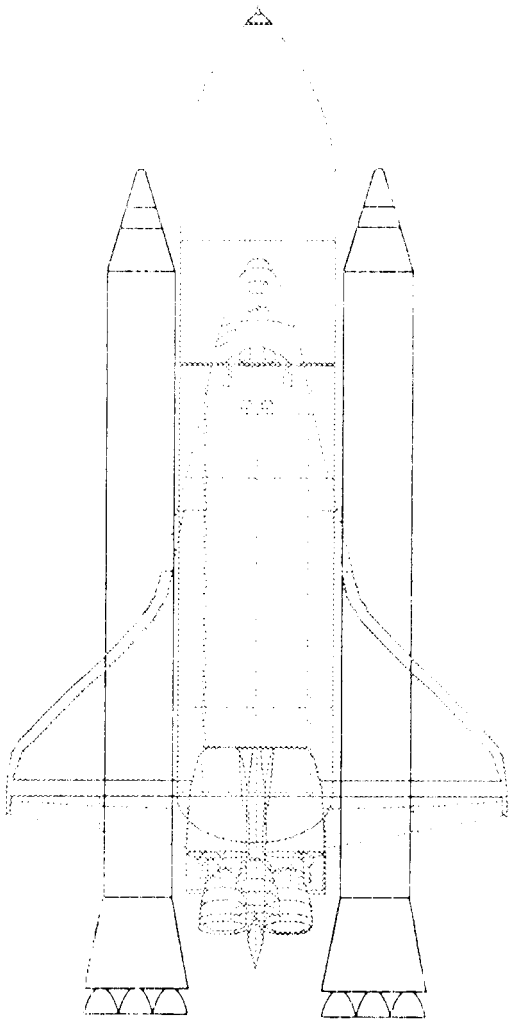

L-C04/jer

MARTIN MARIETTA
MANNED SPACE SYSTEMS

Liquid Rocket Booster Ascent Acoustic and Thermal Environments Remtech Report RTN 186-02

Appendix B

Contents

List of Figures

List of Tables

Section 1
INTRODUCTION

This report describes the ascent thermal environment and propulsion acoustic sources for the Martin-Marietta Corp. designed Liquid Rocket Boosters (LRB) to be used with the Space Shuttle Orbiter and External Tank. Two designs have been proposed: one using a pump-fed propulsion system and the other using a pressure-fed propulsion system. Both designs use LOX/RP1 propellants, but differences in performance of the two propulsion systems produce significant differences in the proposed stage geometries, exhaust plumes, and resulting environments.

The balance of this section will describe the general characterstics of the two designs which are significant for environment predictions. This section will be followed by sections describing the methods of analysis and predictions for environments in acoustics, aerodynamic heating, and base heating (from exhaust plume effects). The acoustic section will compare the proposed exhaust plumes with the current SRB from the standpoint of acoustics and ignition overpressure. The sections on thermal environments will provide details of the LRB heating rates and indications of possible changes in the Orbiter and ET environments as a result of the change from SRBs to LRBs.

Both LRB designs use 4 engines with throttling capability to offer a measure of operation with an engine failure. The significant dimensions of the stages in Figs. 1.1 and 1.2 show the larger size of the pressure-fed stage which results from lower chamber pressure and heavier structure. The booster X and Z axis origins relative to the ET are the same as the current SRB, but the Y axis origin is further from the ET centerline than the 250.5 inches for the SRB because of the larger LRB stage diameters.

The thermal environments were developed for the nominal trajectories in Tables 1.1 and 1.2 and the thrust schedules in Figs. 1.3 and 1.4. The throttle schedules are specified as a fraction of Rated (Emergency) power level. The Pump-Fed stage normally operates at 75-percent of rated power to provide a reserve for throttle-up to compensate for engine failure. The level is further reduced at max-q and near the end of burn to reduce loads and acceleration. Because of the reduced performance of the Pressure-Fed system, it must operate at full power at lift-off, but it drops back to 75-percent throttle at 30 seconds and throttles down late in flight to limit acceleration.

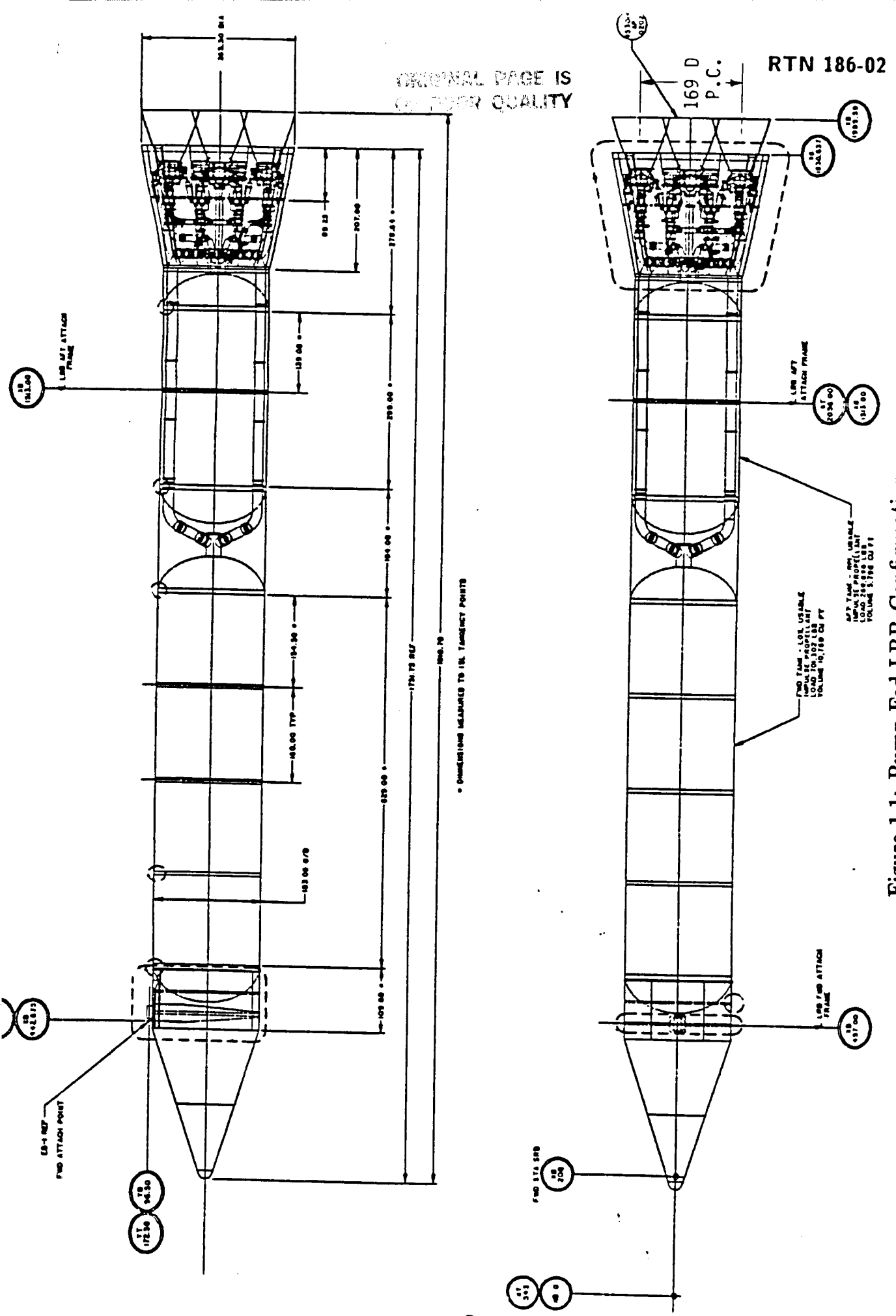

Figure 1.1: Pump-Fed LRB Configuration

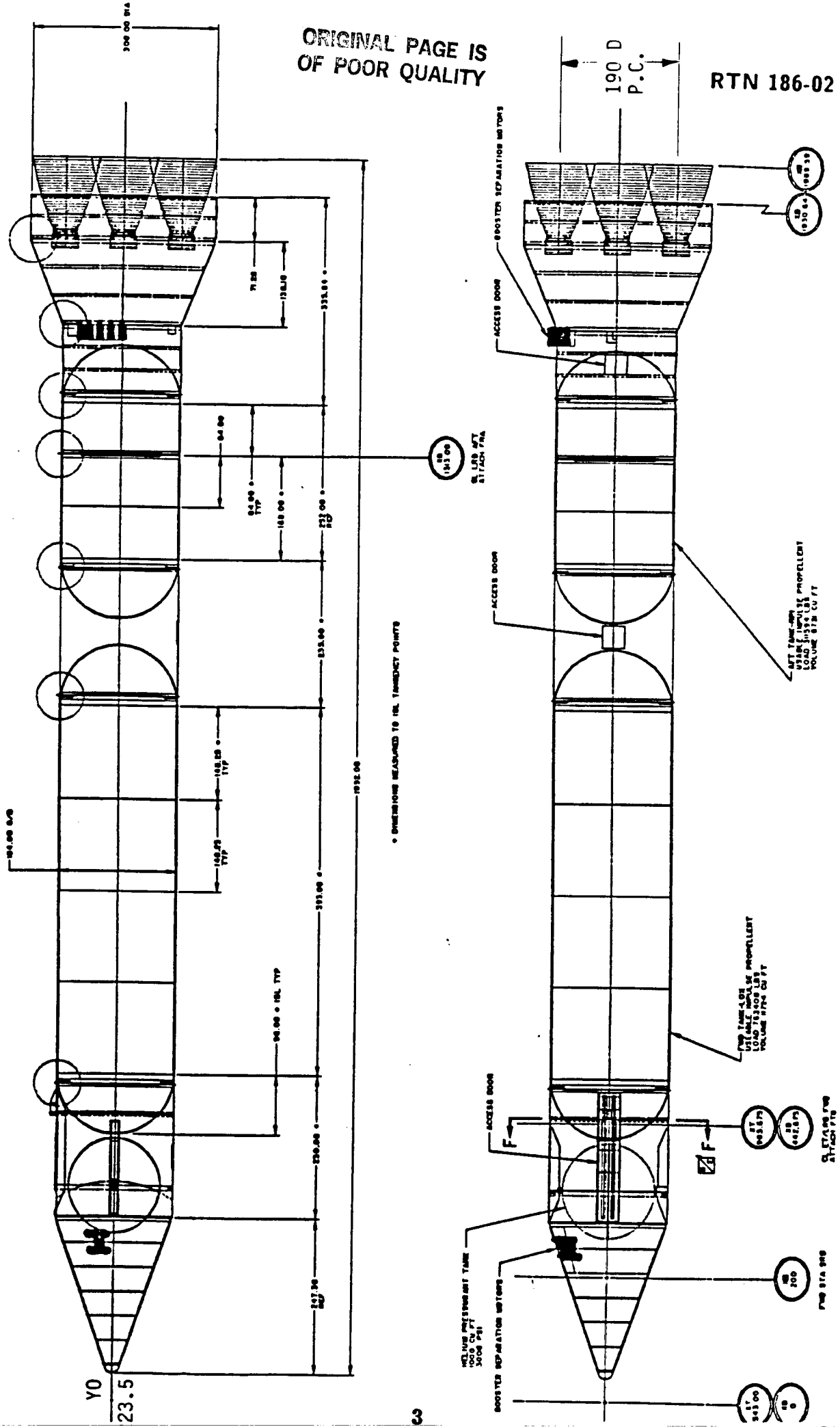

Figure 1.2: Pressure-Fed LRB Configuration

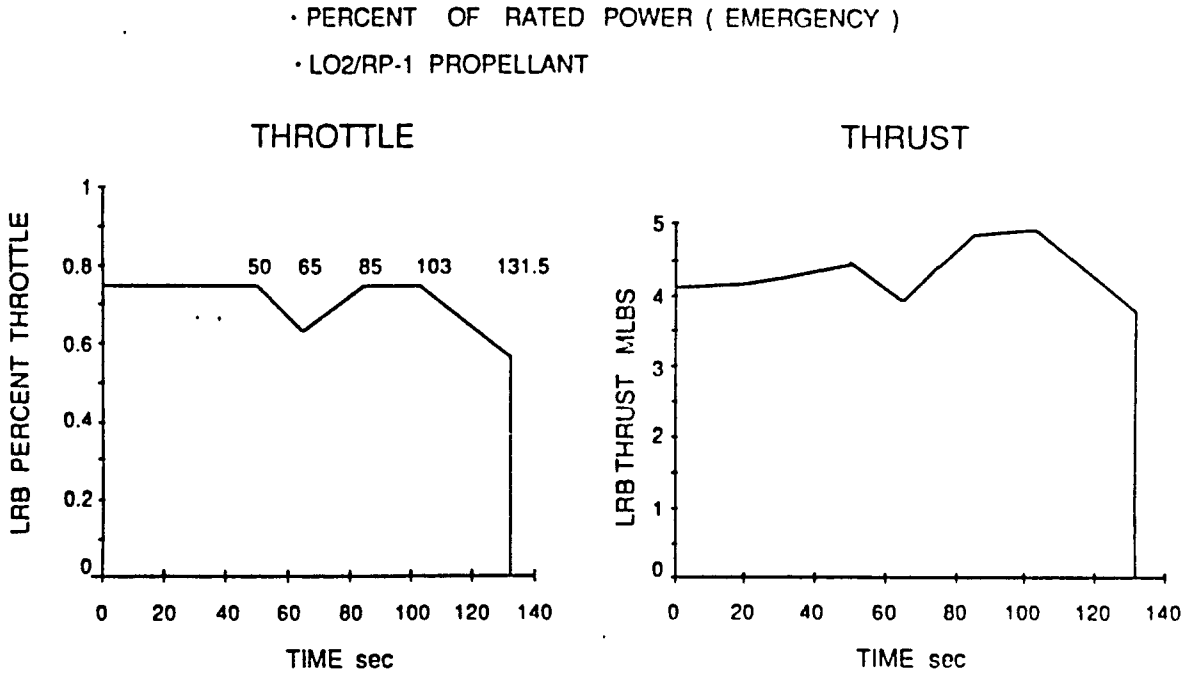

Figure 1.3: Pump-Fed LRB Thrust Schedule

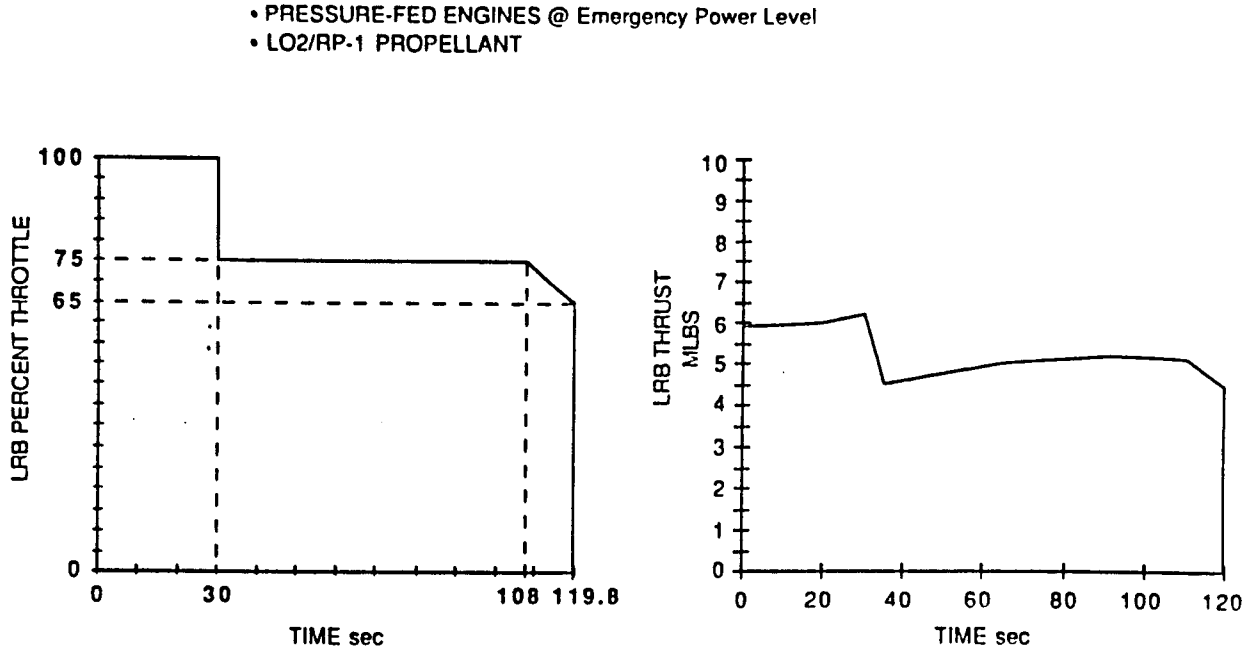

Figure 1.4: Pressure-Fed LRB Thrust Schedule

LRB 70.5K LBS PAYLOAD PERFORMANCE REFERENCE MISSION
PUMP FED BASELINE CONF OF 3-23-88 D.I. WJEIT= 244000
CG 2-22 LOX-RP1 TSL=685K AEROJET 4-4 AERO STS/LRBI OD = 15.3 L=149.5)

TIME (SEC)	ALTITUDE (FT)	MACH NO.	VELOCITYR (FT/SEC)	ALPHA (DEG)	DYNAMIC P (PSF)	QA (PSFD)	ATM. P (PSF)	REYNO	HEATING (BTU/FT2)	GAMMAR (DEG)
.0	95.	.00	.0	90.09	.0	2.	2117.	2.67+006	.0	.000
.3	95.	.00	.0	90.09	.0	2.	2117.	2.67+006	.0	-8.254
.3	95.	.00	.0	-90.09	.0	-2.	2117.	2.67+006	.0	-8.254
6.0	242.	.05	54.1	7.37	3.3	24.	2106.	3.42+007	.0	78.505
6.0	242.	.05	54.1	7.37	3.3	24.	2106.	3.42+007	.0	78.505
10.0	537.	.08	96.5	8.86	10.4	93.	2085.	6.09+007	.0	81.658
20.0	2080.	.19	217.3	4.10	51.5	211.	1975.	1.33+008	.0	84.455
26.0	3618.	.27	306.0	1.56	97.3	152.	1870.	1.81+008	.1	76.236
26.0	3618.	.27	306.0	1.56	97.3	152.	1870.	1.81+008	.1	76.236
30.0	4920.	.33	374.0	.56	138.4	77.	1784.	2.13+008	.1	71.291
35.0	6876.	.42	469.9	-.83	201.9	-169.	1663.	2.52+008	.3	65.901
40.0	9218.	.51	577.8	-2.42	279.9	-678.	1526.	2.90+008	.7	61.701
44.1	11439.	.60	674.4	-3.89	354.1	-1378.	1405.	3.18+008	1.1	59.189
44.1	11439.	.60	674.4	-3.89	354.1	-1378.	1405.	3.18+008	1.1	59.189
45.0	11976.	.62	697.0	-3.91	371.5	-1453.	1377.	3.24+008	1.2	58.738
50.0	15188.	.74	827.5	-4.02	470.9	-1893.	1219.	3.53+008	2.2	56.543
55.0	18884.	.87	963.5	-4.14	565.0	-2338.	1056.	3.72+008	3.7	54.808
60.0	23056.	1.01	1095.5	-4.25	635.9	-2705.	894.	3.80+008	5.9	53.499
65.0	27677.	1.14	1218.3	-4.29	672.8	-2883.	738.	3.75+008	8.8	52.479
70.0	32728.	1.29	1349.3	-4.29	692.0	-2966.	593.	3.63+008	12.5	51.589
75.0	38282.	1.48	1503.9	-4.29	701.0	-3004.	460.	3.46+008	17.1	50.942
80.0	44439.	1.71	1685.4	-3.40	697.6	-2370.	342.	3.18+008	23.0	50.332
85.0	51272.	1.98	1900.6	-1.64	666.2	-1095.	243.	2.74+008	30.7	49.118
90.0	58804.	2.26	2149.1	.30	588.9	179.	165.	2.10+008	40.5	47.109
90.0	58804.	2.26	2149.1	.30	588.9	179.	165.	2.10+008	40.5	47.109
100.0	75818.	2.82	2731.9	2.00	399.1	798.	72.	1.05+008	67.0	41.930
110.0	95308.	3.44	3415.1	2.00	241.4	483.	29.	4.89+007	102.2	37.288
120.0	117102.	4.03	4152.9	2.00	128.1	256.	11.	2.03+007	143.4	33.396
130.0	140926.	4.61	4930.5	2.00	63.8	128.	4.	8.05+006	186.7	30.123
131.5	144620.	4.69	5048.3	2.00	57.4	115.	4.	7.02+006	193.2	29.683
131.5	144620.	4.69	5048.3	2.00	57.4	115.	4.	7.02+006	193.2	29.683
133.9	150584.	4.69	5073.6	1.42	45.5	65.	3.	5.48+006	203.1	29.139
133.9	150584.	4.69	5073.6	1.42	45.5	65.	3.	5.48+006	203.1	29.139
143.9	174733.	4.87	5236.4	9.31	19.6	183.	1.	2.32+006	235.8	26.703
143.9	174733.	4.87	5236.4	9.31	19.6	183.	1.	2.32+006	235.8	26.703
150.0	188863.	5.08	5347.7	8.27	12.2	101.	1.	1.46+006	251.1	25.106
200.0	285481.	7.35	6525.8	1.81	.2	0.	0.	3.07+004	309.2	14.208
250.0	349506.	7.92	8148.3	-1.34	.0	0.	0	9.06+002	322.8	6.813
250.0	349506.	7.92	8148.3	-1.34	.0	0.	0.	9.06+002	322.8	6.813
300.0	382728.	8.56	10214.5	-2.05	.0	0.	0	2.01+002	330.6	2.094
300.0	382728.	8.56	10214.5	-2.05	.0	0.	0	2.01+002	330.6	2.094
350.0	388538.	10.44	12774.5	-3.17	.0	0.	0.	1.93+002	341.4	-.472
400.0	375874.	13.84	15962.2	-2.87	.0	0.	0.	4.39+002	365.8	-1.241
450.0	359876.	18.96	20097.2	-1.63	.0	0.	0.	1.32+003	436.6	-.576
496.4	361435.	22.98	24508.3	-.25	.1	0.	0.	1.48+003	591.8	.810

Table 1.1: Pump-Fed LRB Design Trajectory

LRB 70.5K LBS PAYLOAD PERFORMANCE REFERENCE MISSION
PRESSURE FED BASELINE CONF OF 2-19-88 D.I.
CG 2-22-88 LOX-RP1 AERO STS/LRB(OD = 16.2 L=159.1)

TIME (SEC)	ALTITUDE (FT)	MACH NO.	VELOCITYR (FT/SEC)	ALPHA (DEG)	DYNAMIC P (PSF)	QA (PSFD)	ATM. P (PSF)	REYND	HEATING (BTU/FT2)	GAMMAR (DEG)
.0	95.	.00	.0	90.09	.0	2.	2117.	2.67+006	.0	.000
.3	95.	.00	.0	90.09	.0	2.	2117.	2.67+006	.0	-8.254
.3	95.	.00	.0	-90.09	.0	-2.	2117.	2.67+006	.0	-8.254
6.0	395.	.09	107.9	2.99	13.2	39.	2095.	6.84+007	.0	84.800
6.0	395.	.09	107.9	2.99	13.2	39.	2095.	6.84+007	.0	84.800
10.0	988.	.17	169.9	6.52	40.3	263.	2052.	1.19+008	.0	88.741
20.0	3954.	.38	422.6	5.88	183.2	1077.	1847.	2.48+008	.2	72.296
20.0	3954.	.38	422.6	5.88	183.2	1077.	1847.	2.48+008	.2	72.296
28.6	8224.	.60	675.7	-3.89	398.9	-1552.	1583.	3.49+008	.9	61.810
28.6	8224.	.60	675.7	-3.89	398.9	-1552.	1583.	3.49+008	.9	61.810
30.0	9072.	.64	719.8	-3.93	440.0	-1728.	1534.	3.64+008	1.1	61.304
35.0	12404.	.73	814.6	-4.01	503.9	-2019.	1355.	3.75+008	2.2	59.319
40.0	16092.	.83	918.6	-4.10	566.5	-2321.	1178.	3.83+008	3.6	57.679
45.0	20182.	.94	1033.1	-4.20	625.4	-2626.	1004.	3.87+008	5.6	56.441
50.0	24713.	1.07	1154.0	-4.28	671.0	-2872.	835.	3.84+008	8.1	55.609
55.0	29714.	1.21	1281.4	-4.29	698.0	-2992.	676.	3.75+008	11.5	55.015
60.0	35229.	1.38	1421.3	-4.29	706.1	-3026.	530.	3.58+008	15.6	54.581
65.0	41319.	1.57	1576.0	-4.16	689.0	-2865.	398.	3.31+008	20.8	54.302
70.0	48042.	1.81	1749.8	-2.84	652.5	-1852.	286.	2.89+008	27.2	53.691
75.0	55422.	2.05	1947.1	-1.17	576.2	-675.	196.	2.30+008	35.2	52.378
80.0	63460.	2.28	2170.2	.42	473.6	201.	131.	1.64+008	44.6	50.414
85.0	72139.	2.51	2418.5	2.00	377.3	755.	86.	1.13+008	55.5	48.040
90.0	81442.	2.75	2691.7	2.00	292.6	585.	55.	7.72+007	67.7	45.615
90.0	81442.	2.75	2691.7	2.00	292.6	585.	55.	7.72+007	67.7	45.615
100.0	101970.	3.30	3313.4	2.00	165.5	331.	22.	3.40+007	95.7	41.236
110.0	125165.	3.86	4038.5	2.00	84.4	169.	8.	1.35+007	127.2	37.484
119.8	150414.	4.43	4795.0	2.00	40.9	82.	3.	5.22+006	159.4	34.377
119.8	150414.	4.43	4795.0	2.00	40.9	82.	3.	5.22+006	159.4	34.377
120.0	151050.	4.43	4796.1	1.94	39.9	78.	3.	5.08+006	160.2	34.324
122.2	156873.	4.42	4806.2	1.42	31.9	45.	2.	4.02+006	166.8	33.831
122.2	156873.	4.42	4806.2	1.42	31.9	45.	2.	4.02+006	166.8	33.831
132.2	183074.	4.65	4941.7	18.31	12.9	237.	1.	1.64+006	190.8	31.087
132.2	183074.	4.65	4941.7	18.31	12.9	237.	1.	1.64+006	190.8	31.087
150.0	225966.	5.34	5241.3	13.67	2.7	38.	0.	3.76+005	216.6	25.548
200.0	319391.	6.85	6442.9	3.90	.0	0.	0.	3.96+003	240.3	19.361
250.0	376059.	7.01	8103.8	-1.61	.0	0.	0.	2.21+002	246.1	5.625
270.7	389759.	7.24	8915.6	-2.93	.0	0.	0.	1.28+002	248.0	3.441
270.7	389759.	7.24	8915.6	-2.93	.0	0.	0.	1.28+002	248.0	3.441
300.0	400437.	7.71	10192.1	-4.09	.0	0.	0.	8.56+001	251.0	1.151
350.0	398858.	9.78	12757.2	-4.60	.0	0.	0.	1.16+002	259.2	-1.045
385.0	387148.	12.26	14911.1	-4.16	.0	0.	0.	2.40+002	271.5	-1.569
385.0	387148.	12.26	14911.1	-4.16	.0	0.	0.	2.40+002	271.5	-1.569
400.0	380689.	13.51	15948.9	-3.93	.0	0.	0.	3.46+002	280.4	-1.576
450.0	361051.	18.88	20087.2	-2.59	.0	0.	0.	1.24+003	347.2	-.717
496.6	361435.	22.99	24508.6	-1.18	.1	0.	0.	1.48+003	501.7	.810

Table 1.2: Pressure-Fed LRB Design Trajectory

Because of the importance of the propulsion system characteristics in the evaluation of acoustics and base thermal environments, predictions were made for 1-D plume characteristics using the Lewis CEC code.. Results of the 1-D predictions for the LRB engines at two power levels and two useful comparison engines are shown in Table 1.3. The data include both exit conditions and conditions assuming an isentropic compression (or expansion) to 1-D flow at sea level pressure. Since the LRB nozzles are overexpanded at sea level, a compression will occur which will not be isentropic, but the 1-D isentropic condition gives a measure of the relative plume size and temperature when compressed. As indicated in the thrust schedules (Figs. 1.3 and 1.4), the engines will always operate at a specified power level for liftoff, so characteristics for the 1-D plumes expanded to sea level are only provided for the lift-off power levels in Table 1.3.

Although the 1-D pressure and temperature for the nozzle exit are usually lower than actually occur at the nozzle lip in the axisymmetric (2-D) nozzle flow, they are useful of comparative purposes. Some predictions for the actual lip pressure are also included in the table to indicate more realistic conditions.

At the time these analyses were made a complete description of the handling of the exhaust gases from auxiliary systems were not available, so the following reasonable assumptions have been made:

- The pump-fed engine will use regenerative cooling for the combustion chamber and an initial portion of the nozzle, and the turbopump exhaust gases will be injected into the nozzle at the termination of the regeneratively cooled portion.
- The pressure-fed engine will use a heat exchanger for pressurant gas, the exhaust gases will be dumped from a mast at the most outboard point at the aft edge of the booster skirt (to prevent recirculation into the base region).

CHARACTERISTIC	S-IC F-1	SRB	PUMP-FED LRB EPL	PUMP-FED LRB NPL	PRESSURE-FED LRB EPL	PRESSURE-FED LRB NPL
PROPELLANTS	LOX/RP1	SOLID	LOX/RP1	LOX/RP1	LOX/RP1	LOX/RP1
O/F RATIO	2.27	-	2.50	2.61	2.67	2.67
CHAMBER CONDITIONS						
Pressure (psia)	965	900	1300	1033	800	630
Temperature (R)	6426	6129	6658	6637	6588	6511
LIFT-OFF THRUST						
Engine	1.5 M	3.0 M	0.685 M	0.513 M	0.750 M	0.562 M
Stage	7.5 M	3.0 M	2.74 M	2.05 M	3.0 M	2.25 M
ENGINE NOZZLES						
Area ratio	16.0	7.7	21.2	21.2	15.4	15.4
Exit press (2)	9.85		7.76	5.88		
Exit Dia. (in.)	140	149.6	96.8	96.8	109.2	109.2
STAGE NOZZLES						
Number of nozzles	5	1	4	4	4	4
Eff. De (in.) (1)	313	149.6	193.6	193.6	218.4	218.4
1-D NOZZLE EXIT						
Pressure (psia)	6.16	19.4	5.94	4.77	5.71	4.25
Temperature (R)	2806	4064	2869	2912	3161	3118
Velocity (fps)	10060	8125	10312	10264	9946	9918
Stage Acoustic						
Power (MW)(3)	255.8	82.6	95.8	71.4	101.2	75.6
(dB)(4)	204.1	199.2	199.8	198.5	200.0	198.8
f / f(SRB)(5)	0.59	1.00	0.98	0.98	0.84	0.84
1-D SEA LEVEL (6)						
Plume Dia. (in)	101.7	166.0	N/A	63.6	76.9	N/A
Temperature (R)	3323	3988	N/A	3587	3757	N/A
Velocity (fps)	9468	8353	N/A	9515	9262	N/A
Stage Acoustic						
Power (MW)(3)	240.7	85.0	N/A	66.2	94.2	N/A
(dB)(4)	203.8	199.3	N/A	198.2	199.7	N/A
f / f(SRB)(5)	0.83	1.00	N/A	1.49	1.20	N/A

NOTES:
1. Effective stage exit dia.
   $De = \text{nozzle exit dia} * \sqrt{\text{number of engines}}$.
2. Estimated axisymmetric prediction of wall pressure.
3. Acoustic power of the stage in watts assuming 0.5 percent conversion of mechanical to acoustic power using 1-D velocity prediction for each condition.
4. Acoustic power expressed in dB relative to 10e-12 watts.
5. Acoustic spectra for rocket exhaust are normally nondimensionalized using the Strouhal number (f De / Ue), where the effective diameter (Note 1) is used. The resulting relative frequency ratio is :
   $f / f(SRB) = [De/Ue](SRB) / [De/Ue]$.
6. Isentropic expansion from the chamber to sea-level pressure.

Table 1.3: Propulsion System Comparisons

Section 2
ACOUSTIC AND OVERPRESSURE

The acoustic and ignition overpressure environments for the two LRB designs will be reviewed in this section. The acoustic levels for the LRB are expected to be comparable to the current SRB, but the ignition overpressure loads for the LRB will be negligible.

2.1 Overpressure

Extensive overpressure analysis and testing during the Space Shuttle development led to the conclusion that the strength of an overpressure wave from engine ignition is primarily a function of the chamber pressure rise rate with appropriate corrections for chamber pressure and geometric scale. For two configurations, the magnitude of an overpressure pulse can be estimated from

$$dp1/dp2 = [(L1 * \dot{P}r1)^2 \ /Pc1]/[(L2^2 * \dot{P}r2) \ /Pc2] \qquad (2.1)$$

where: dp = overpressure amplitude
L = length scale for the engine
$\dot{P}$r = maximum chamber pressure rise rate
Pc = champer pressure level at Pr

The approximate values for the SRB parameters in the above equation are: $\dot{P}$r = 8500 psi/sec, Pc = 200 psia, and L = 150 inches (nozzle exit diameter).

The rise rate of the LRB engines is expected to be comparable to other large liquid rockets, so typical F-1 starting data have been used to represent the LRB engines. The F-1 engine starting was staggered and the rise rate for each was about 1000 psi/sec at chamber pressures as low as 100 psi.

The LRB engines have exit diameters less than 75 percent of the SRB, and although there are four nozzles rather than one as on the SRB, it is expected that the engine ignitions will be staggered by a fraction of a second to limit ignition loads.

Regardless of the length scale used, the low pressure rise rates of liquid rocket

engines will produce much lower overpressure potential. For the approximate LRB characteristics described above, the predicted ratio of LRB to SRB overpressure pulse is

$$\begin{aligned} dp(LRB)/dp(SRB) &= [(0.75 * 1000)^2/100]/[(1.0 * 8500)^2/200] \\ &= 0.016 \end{aligned}$$

Based on this result, the overpressure is expected to be negligible, and it is unlikely that either changes in the starting sequence or changes in the starting characteristics of LRB engines relative to the F-1, could produce levels approaching the current SRB levels.

2.2 Acoustics

It is difficult to define the acoustic characteristics of a new stage, but the acoustic parameters of engines and stages can be compared to indicate the expected relative changes in power level and spectra. Considering the similarity of the SRB and LRB acoustic parameters, it is expected that the differences between the two stages will be much less than the errors involved in predicting the acoustic level of the LRB independently. Because of this, the acoustic analysis has been approached as an incremental comparison. But even this approach cannot be carried to the logical conclusion of adjusting the SRB spectra by the predicted increments because the current acoustic spectrum of the SRB is not available. It is combined with the SSME which are ignited first in the launch sequence.

Acoustic levels are usually highest at launch when the vehicle velocity is zero and the launch stand deflects the gases so that the sound radiates more in the direction of the vehicle. During Space Shuttle launches large amounts of water are used to decrease acoustic and overpressure levels. The maximum acoustic levels occur on the pad for base regions primarily due to the SSME source, but as the vehicle rises and the SRB plumes come out from beneath the launch platform, acoustic levels at positions in the cargo bay area increase. The maximums occur at altitudes of 60 to 120 feet above the pad as the SRB plumes impinge on the launch platform.

A comparison of various stages has shown that the overall acoustic power of a stage is proportional to the mechanical power (thrust * exhaust velocity / 2) of the stage with conversion efficiencies in the range of 0.2 to 1.0 percent. The relative acoustic power for the SRB and LRB stages are listed in Table 1.3 for two

conditions. The nozzle exit condition is often specified as the proper parameter to use in the power, but the fully expanded velocity is recommended in Ref. [1]. This provides a conservative and realistic accounting for the increase in velocity of underexpanded nozzles just outside the nozzle. In the case of the over-expanded LRB nozzles, the expansion to sea-level pressure is actually a compression from the nozzle exit condition. This results in lower acoustic power at the launch power levels on the two LRB stages.

Since the scale and configuration of the SRB and LRB acoustic sources are similar, changes in sound power level of the plumes is a reasonable approximation for changes in sound pressure level. If the maximum of the acoustic power (nozzle exit or fully expanded) from Table 1.3 is used for each stage, the following estimates are are obtained for the change in the overall sound pressure level at launch:

Pump-Fed (NPL) - SRB = 198.5 - 199.3 = −0.8 dB
Pressure-Fed (EPL) - SRB = 200.0 - 199.3 = +0.7 dB

If it is conservatively assumed that the SRB source is much stronger than the SSME, the estimates above represent the anticipated change in the overall acoustic level.

Even though the overall pressure level represents only a slight change, the likely effect on the spectra must be considered to evaluate the effect on the Shuttle structure. The Strouhal number is the dimensionless parameter relating the frequence spectra with the vehicle parameters. It is defined as:

$$\text{Strouhal number} = f\,De\,/\,Ue$$

where: f = frequency (Hz),
De = effective nozzle diameter (ft), and
Ue = effective exhaust velocity (ft/sec).

The effective nozzle diameter for a multiple engine stage is normally taken to be the effective diameter of a single similar engine with the same thrust. This gives

$$De = \sqrt{n}\;\; Dn$$

where: n = number of nozzles, and
Dn = diameter of one of the nozzles.

The ratios of LRB to SRB frequencies are included in Table 1.3 for both the nozzle exit and fully expanded (or compressed) condition at sea level. Test ratios indicate that the spectra of the LRB stages relative to the SRB could shift by ratios of 0.84 to 1.49 depending on the stage and velocity condition selected.

The condition usually recommended, with expansion or compression to sea-level pressure, indicates that the spectrum of the LRB vehicle will be shifted to slightly higher frequencies with a ratio of 1.49 for Pump Fed and 1.20 for Pressure Fed. Ratios in this range, less than 1/2-octave, are not considered significant.

Section 3
ASCENT AERODYNAMIC HEATING

A preliminary assessment of aerodynamic heating to the pressure-fed and pump-fed launch systems was made and the results are reported in this section. The data reported in this section compare relative heating between the two LRB systems and the baseline Shuttle systems.

3.1 Comparison of LRB with Baseline Shuttle Ascent Trajectories

The ascent trajectory parameters for the LRB study baseline pump-fed and pressure-fed systems were given in Tables 1.1 and 1.2. These trajectories are non-dispersed mean reference trajectories launched from ETR with the objective of delivering up to 70,500 pounds of payload to LEO. The ascent thermal design trajectory for the baseline STS was a 3 σ dispersed (hot) trajectory that assumed an engine failure at $\approx$ 260 seconds which simulates the AOA abort case. The STS design trajectory is launched from WTR to perform a 3A mission. Figure 3.1 compares the altitude/velocity profiles for the two LRB reference trajectories with the STS reference and dispersed trajectories. This figure shows that the LRB ascent trajectories are very similar to the baseline reference STS trajectory.

3.2 Comparison of Heating Indicator Results

Heating results for the stagnation point of a one-foot sphere were calculated for each of the four trajectory profiles. Based on Shuttle and previous flight vehicle programs, the use of this heating indicator to compare relative trajectories from an aeroheating standpoint has proven to be acceptable. A comparison of heating indicator results for all four trajectories are given in Table 3.1. This table shows that the pump-fed system will experience $\approx$ 30 percent higher peak heating rates than the pressure-fed system. The heat rate profiles for the STS baseline reference and design trajectories are presented in Figure 3.3. This figure shows that including dispersions and an assumed engine-out abort case (design) increases peak heating by $\approx$ 40 percent. The conclusions drawn from the heating indicator study are summarized in Table 3.2. The heat load comparisons are based on first stage loads

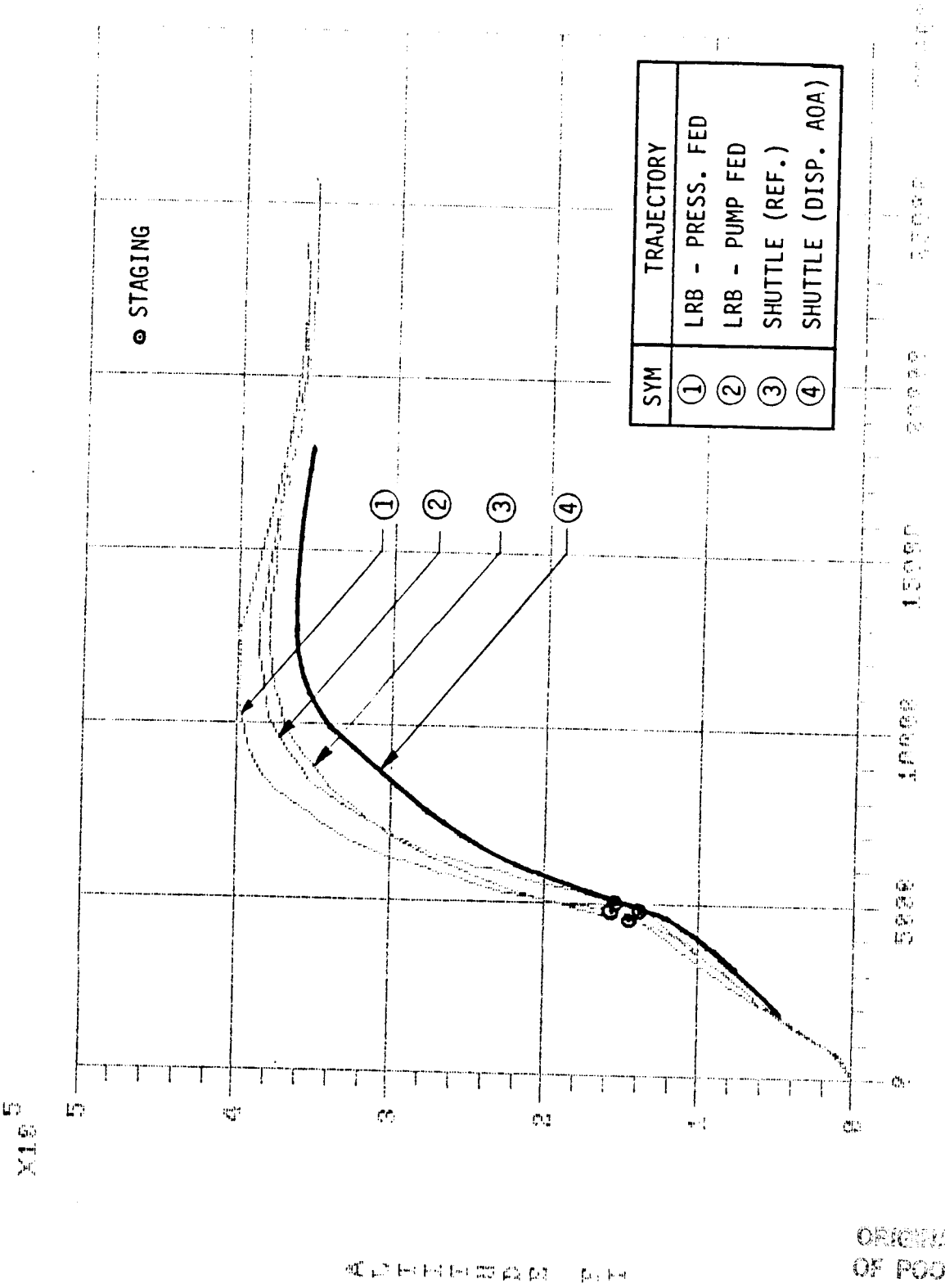

Figure 3.1: Comparison of LRB with Baseline Shuttle Trajectory

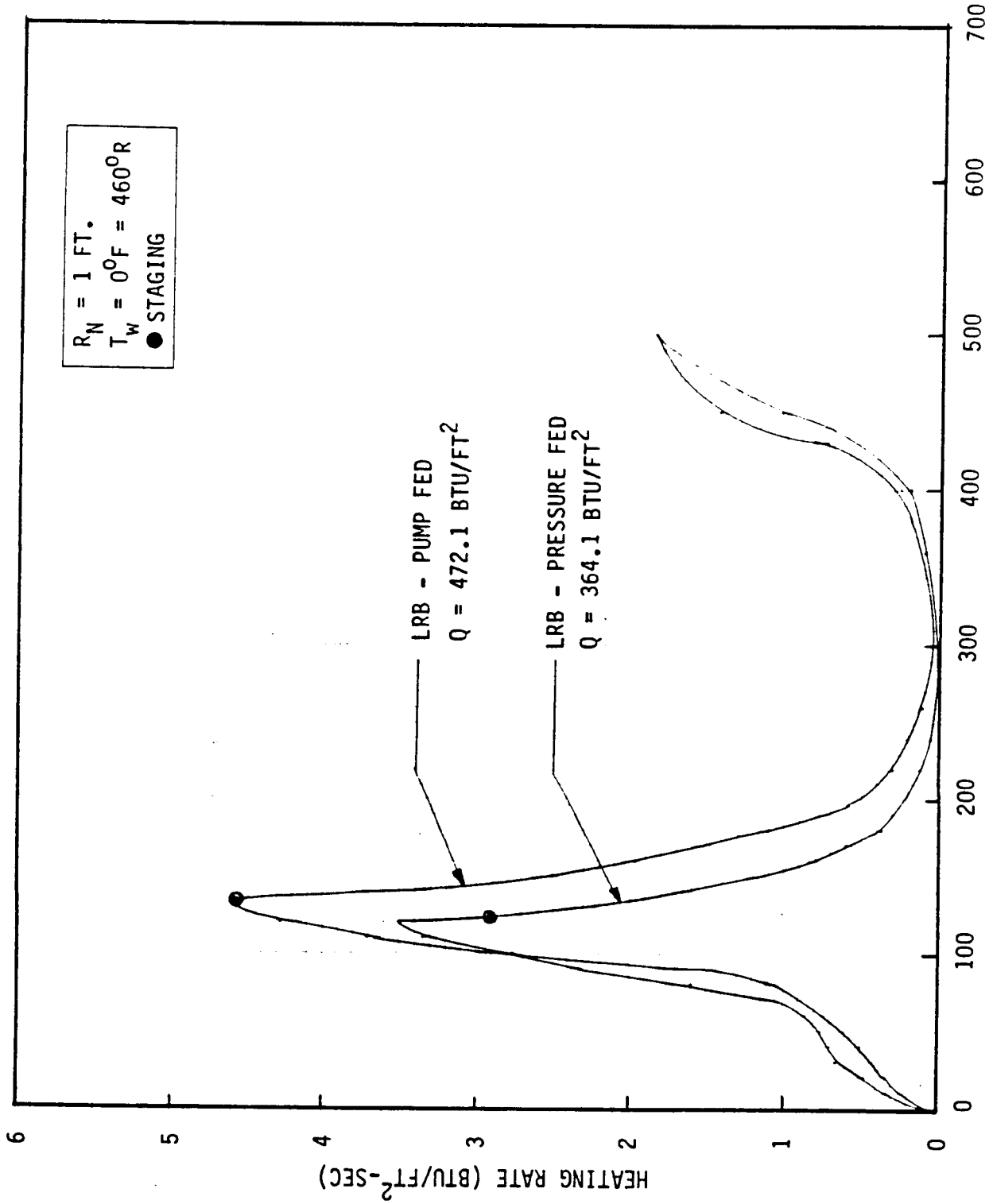

Figure 3.2: Comparison of Heating Indicator Results for Pump-Fed and Pressure-Fed LRB Trajectories

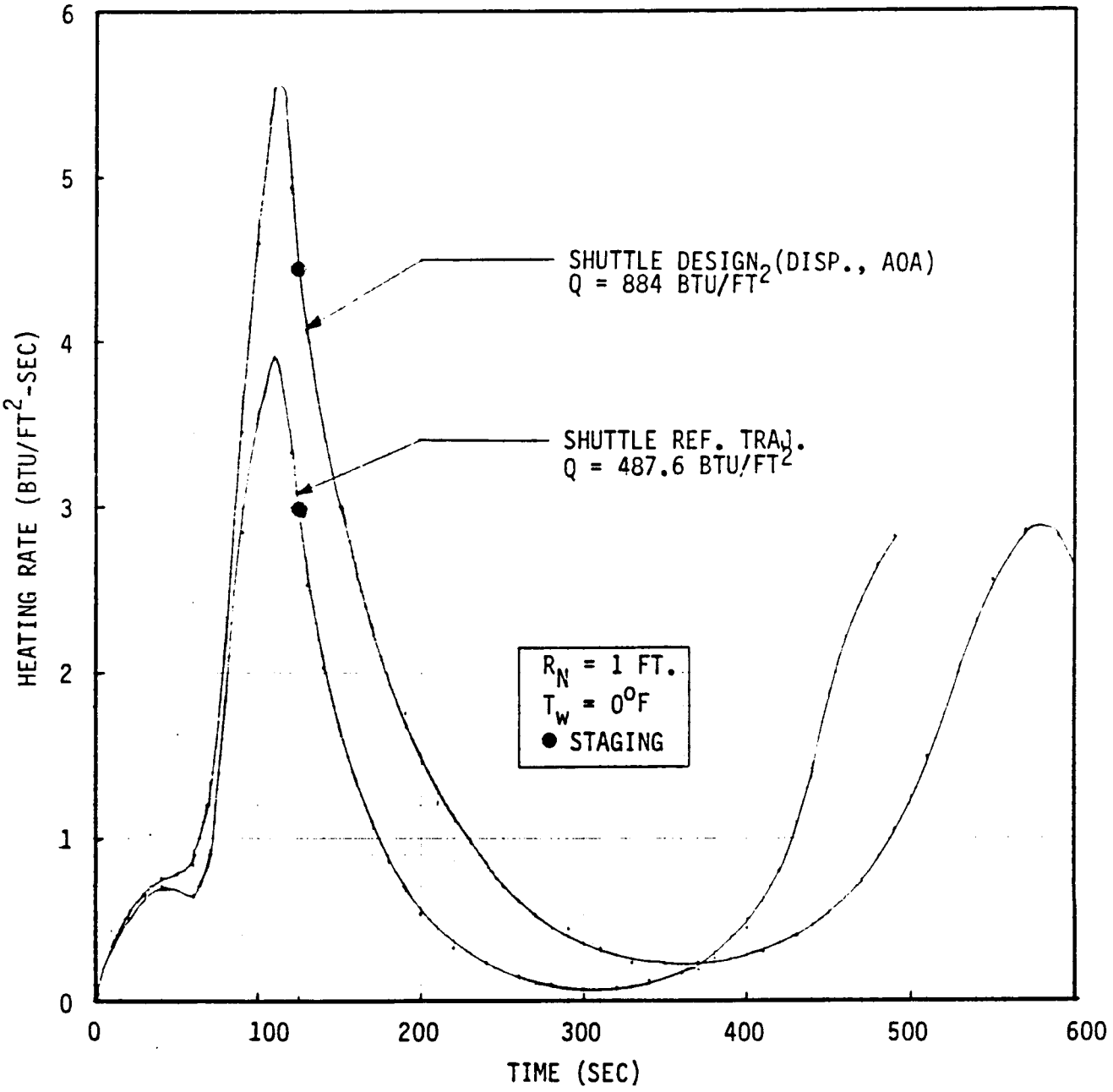

Figure 3.3: Comparison of Heating Indicator Results for Shuttle Reference Mission and Design

- PUMP FED VEHICLES WILL EXPERIENCE HIGHER AERODYNAMIC HEATING THAN PRESSURE FED
  - 15% HIGHER FIRST STAGE HEAT LOAD
  - 30% HIGHER PEAK HEAT RATE
- CURRENT SPACE SHUTTLE AEROHEATING COMPARED TO LRB CONFIGURATIONS (FIRST STAGE)
  - PUMP FED HEATING $\approx$ EQUAL TO SHUTTLE
  - PRESSURE FED HEATING COOLER THAN SHUTTLE (13%)
- COMPARISON OF SHUTTLE BASELINE REFERENCE TRAJECTORY WITH THERMAL DESIGN DISPERSED TRAJECTORY SHOWED THAT DISPERSIONS INCREASED ASCENT AEROHEATING BY 40%
- ASCENT AEROHEATING DIFFERENCES BETWEEN LRB AND CURRENT SHUTTLE NOT CONSIDERED LARGE ENOUGH TO SIGNIFICANTLY IMPACT CURRENT TPS MATERIALS OR APPLICATION PROCEDURES

Table 3.2: Conclusions Drawn from Aeroheating Indicator Results

since heating indicator comparisons tend to be more realistic using the first stage loads, and the results are intended for LRB preliminary design use. The heating experienced during second stage flight after 150 seconds is relatively low with the exception of the tip region of the ET nose.

3.3 Potential Impacts of LRB Configurations to ET and Orbiter

The only potential design impact of the LRB systems on the TPS design of either the Orbiter or the ET will most likely be the pressure-fed LRB system on the ET sides. Relative to the ET, the nose of the pressure-fed LRB is $\approx$ 63 inches further forward than the current baseline STS SRB. This results in the bow shock of the pressure-fed LRB impinging directly on the LO_2 tank rather than on the intertank for the baseline. The current TPS (CPR-488) thickness on the LO_2 tank in this shock impingement region is $1.0'' \pm .25''$. The heating will amplify significantly in the region of $X_T \cong 750$ to 852 along each side of the LO_2 tank. The peak heating in this shock impingement region is expected to increase from $\approx$ 2.2 Btu/ft^{2}sec to 12-15 Btu/ft^{2}sec. The issue is whether film boiling of the liquid oxygen along the sides of the LO_2 tank occurs. The CPR-488 thickness will probably have to be increased from the $1.0'' \pm .25''$ to protect the side of the LO_2 tank from the amplified heating. It is recommended that MMC conduct a thermal analysis for the baseline body point 71775 ($X_T = 796.5$, $\theta_T = 270°$). The baseline design environment for this body point should be multiplied by a factor of 7 from 60 seconds until LRB separation time. The shock impingement region on the ET for the pump-fed system is expected to still be on the intertank which should not result in a TPS impact.

Section 4
BASE HEATING

4.1 Introduction

The base heating environment consists of radiative and convective components. Infrared radiation from the rocket exhaust plumes varies strongly with surface position as views of the plumes from the surface and shading by other surfaces change. In contrast, the convective heating environment, resulting from reversed plume boundary layer gases, is specified as relatively constant over wide areas. Both heating modes are basically a function of altitude, with flight-time effects also entering through variations in engine thrust. In this application, all environments have been converted to time histories for environment specifications by using the design trajectories in Tables 1.1 and 1.2.

At launch, the primary heat source is radiation from the rocket exhaust plumes. As altitude increases, the radiation changes depending on the plume characteristics. It may increase slightly as bright opaque plumes (e.g. LOX/RP1 or SRB) expand, or decrease rapidly as relatively transparent gas plumes (e.g. LOX/H2 or N2O4/MMH) expand and cool. At an altitude which is a function of engine arrangement and nozzle lip pressure, portions of the plume boundary layer flow begin to reverse toward the base. This process often increases until reversed plume flow fills relatively large portions of separated regions around the base. This extends the area effected by convective heating and causes an increase in radiation as the new radiation source grows.

In the current Space Shuttle, the increase in radiation associated with reversal into the ET base region before booster separation is not a significant factor in the thermal load. However, on the Saturn S-I stage and to a greater extent on the Saturn S-IC stage, radiation from the reversed gas was significant and increased base radiation rates 2 to 3 times above the sea-level values. It appears that this increased significance is a result of the increased emissivity of the reversed gas because of the soot produced in LOX/RP1 plumes.

Because of the inability to predict the size of separated flow regions and the gas properties in the regions, base environment prediction is particularly tenuous for the LOX/RP1 propellants used by the LRB designs. The environment to be presented considers the reversed gas radiation source, but a nominal impact is

projected rather than the worst case experience encountered in the Saturn S-IC.

The base regions selected for analysis include the LRB skirt, base heat shield and nozzles as shown in Fig. 4.1. The heating rates to be presented later correspond to the maximum rate anticipated in each of the regions. The ET base center has been selected to evaluate the LRB in comparison with the current SRB conditions.

The sections below describe the radiative and convective prediction methodologies and predicted thermal environments.

4.2 Radiation

The radiation prediction methodology follows the procedure used for previous LOX/RP-1 plumes and for the current SRB. A plume model of opaque surfaces is developed with assigned emissive powers to provide a sea-level prediction, and an altitude adjustment ratio is applied to the sea-level rate for ascent.

The sea-level plume emission levels are developed initially from previous experience; then improved as measurements of static test firings become available. The dependence on empirical data is caused by the inability to predict either the concentration or the optical properties of the soot particles which result from LOX/RP1 combustion. These particles are not predicted by ideal chemical composition codes because the occurrence of the particles is a result of the real chemical changes in the fuel structure in the combustion process. These changes prevent combustion of some of the carbon.

The most recent large LOX/RP-1 engine which can be used to approximate the LRB engines is the F-1 engine on the Saturn S-IC stage. The sea-level plume model for this engine based on measurements [2] is shown in Fig. 4.2a. The short cold initial portion of the plume is a result of fuel-rich turbine exhaust gases injected into the nozzle at the 10:1 area ratio. These gases are burned fuel-rich to provide a lower temperature for the pump turbines, so they form a relatively cool soot shield over the hotter plume gases. A short distance from the nozzle exit, these gases mix with the plume and air to produce a bright afterburning mantel which is extremely long.

The pump-fed engine at NPL is similar to the F-1 except that it is smaller and has a higher area ratio. It will have turbine exhaust gases injected into the nozzle to form an initial opaque cool boundary followed by a bright afterburning plume. The cooler gas temperature expected by the higher expansion of the LRB engine is offset by the higher O/F ratio to produce plume temperatures comparable to the F-1 (see Table 1.3). The lower exit pressure of the LRB engine will have

CIRCUMFERENTIAL ZONES			
θ_B		θ_N	
0 - 180	180 - 360	-90 - 90	90 - 270
E1	E2	C1	C2
F1	F2		

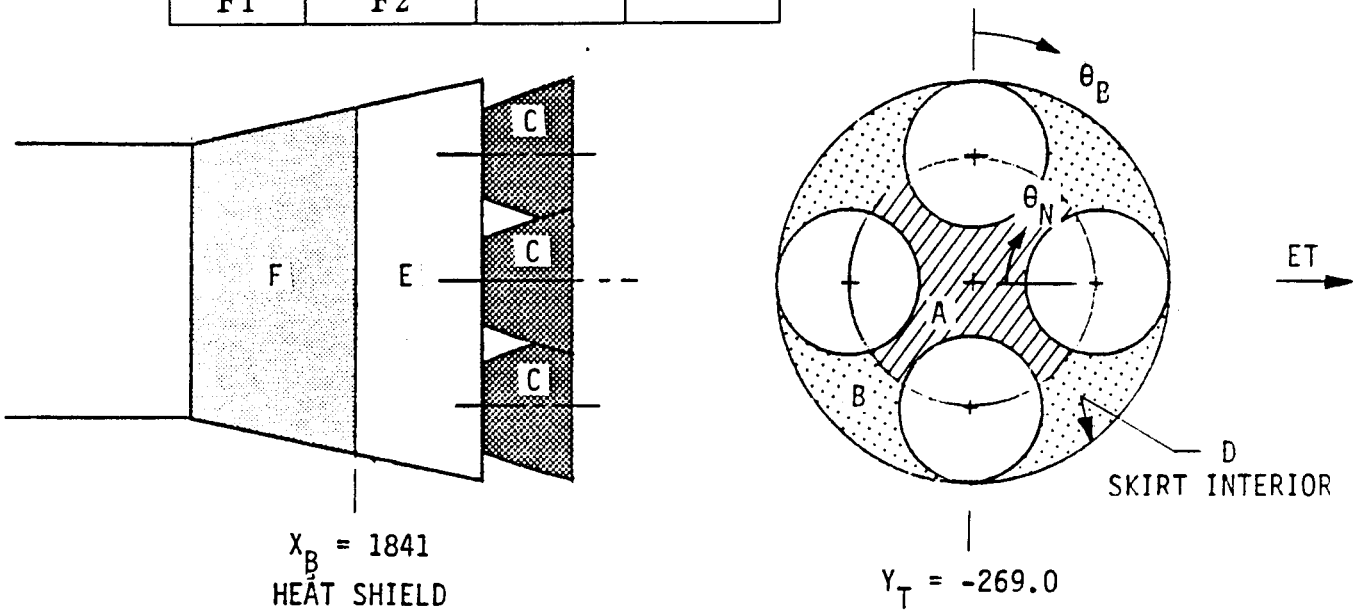

(a) Pump-Fed LRB

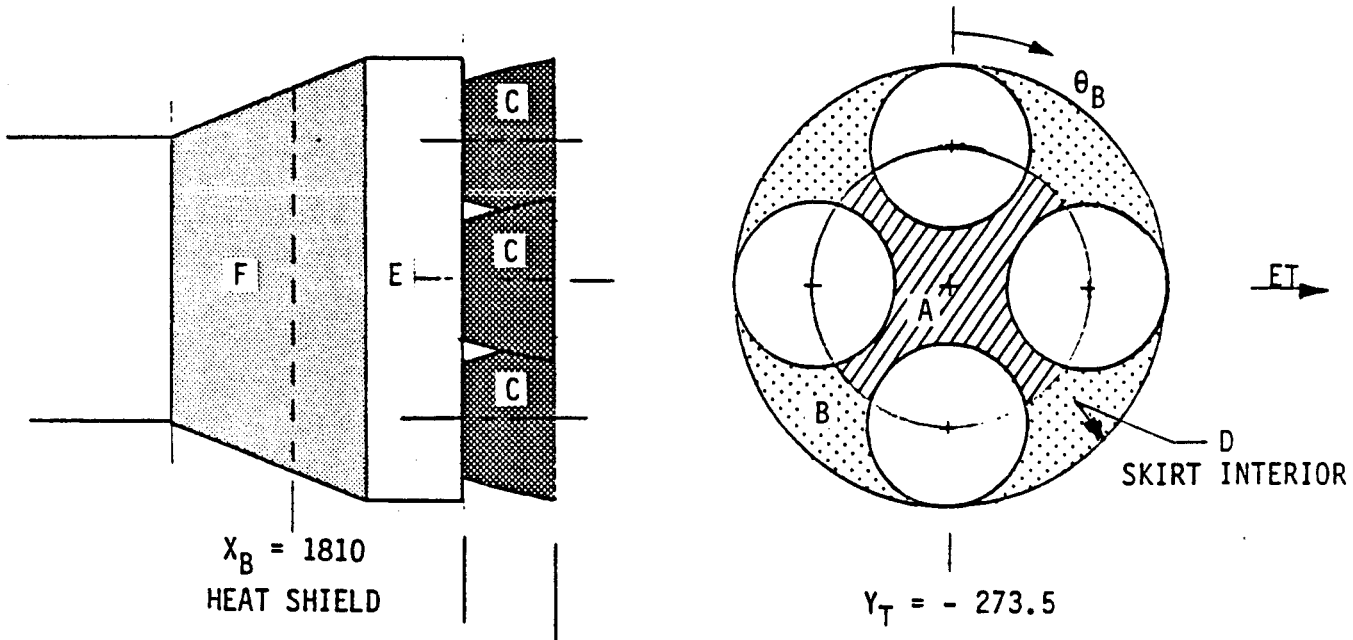

(b) Pressure-Fed LRB

Figure 4.1: Base Environment Regions

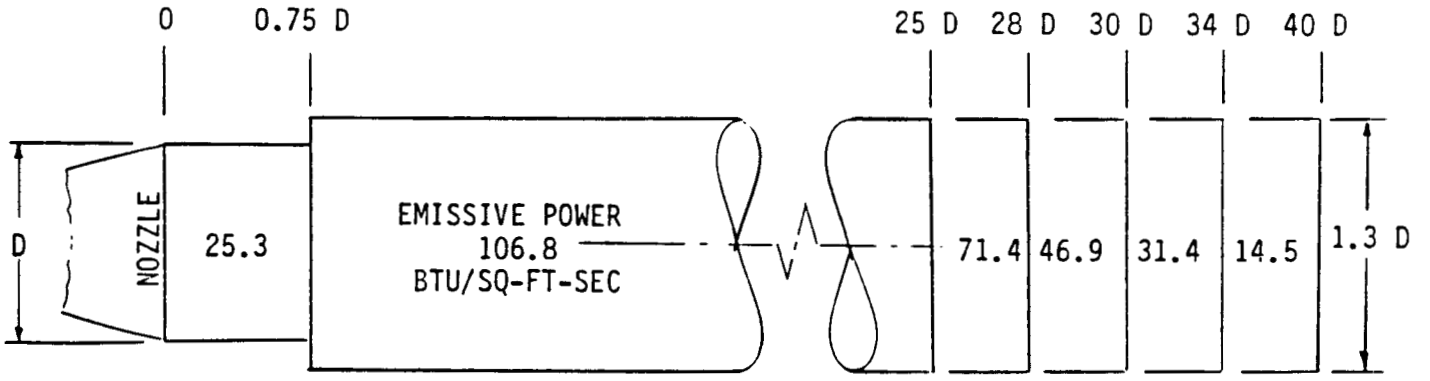

(a) F-1 Engine (D = 140 in.)

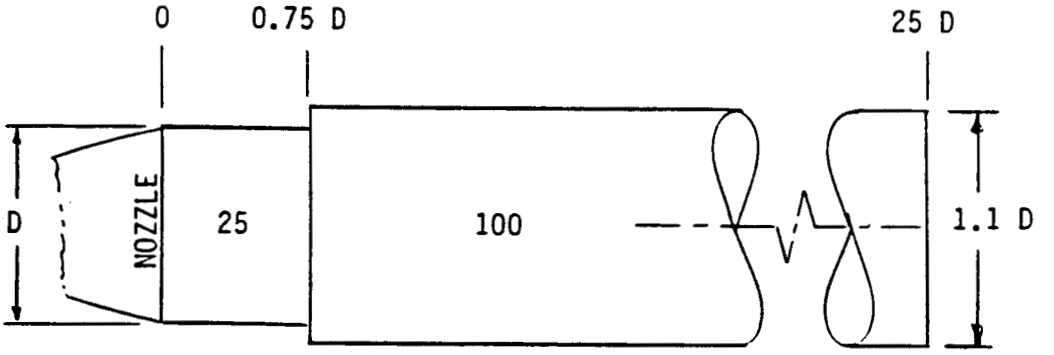

(b) Pump-Fed LRB (D = 96.8 in.)

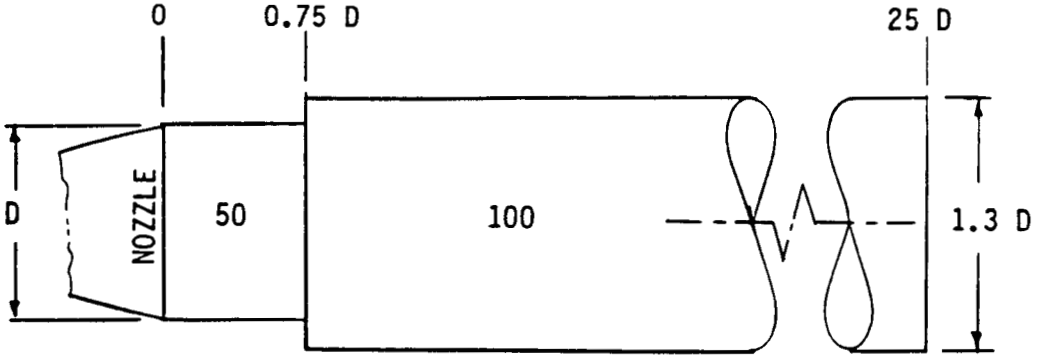

(c) Pressure-Fed LRB (D = 109.2 in.)

Figure 4.2: Sea-level Plume Models for F-1 and LRBs

two effects. The plume will be smaller relative to the nozzle diameter and the shock structure in the near plume will produce higher internal temperatures. The proposed plume model for the pump-fed engine in Fig. 4.2b has a slightly smaller diameter relative to the nozzle because of the greater expansion in the nozzle, and the emissive power is reduced slightly because the higher O/F ratio will produce less soot and fewer afterburning species. It has been assumed that the stronger shock structure in the pump-fed engine plume will be effectively shielded from the base aspect by the opaque turbine exhaust gas. The plume is reduced in length relative to the F-1 engine because the far plume does not have significant influence on the base.

The pressure-fed engine will be at EPL at launch, so this condition (Table 1.3) is considered in designing the plume model. This engine will have no fuel-rich turbine exhaust gas in the nozzle boundary layer, so afterburning is likely to start sooner and the shock structure resulting from the over-expanded nozzle may be more visible. The higher O/F ratio for this engine combined with the reduced expansion (caused by the lower chamber pressure) produces exhaust gases which are hotter than the pump-fed. Since the nozzle exit pressure is comparable to the F-1, the pressure-fed plume-to-nozzle diameter ratio of the F-1 is used, but the cool initial portion is replaced with a hotter one corresponding roughly to the emissive power of a blackbody at the predicted (1-D) nozzle exit temperature. This initial section simulates a short mixing zone before significant afterburning starts. Although the plume temperature expanded to sea level is significantly higher than the F-1 engine, it appears reasonable to retain the F-1 emissive power. The F-1 emissive power is high because of afterburning rather than the plume temperature. The pressure-fed plume radiation model is shown in Fig. 4.2c.

The altitude variation applied to the predictions obtained using the sea-level models must reflect three trends: the variation in thrust of the engines, the reduction in plume temperature by expansion, and the radiation from plume gases reversed into separated regions. The characteristics of each of these trends will be discussed before presenting the altitude adjustments selected for the two LRB stages.

Thrust reduction for the LRBs is accomplished by chamber pressure reduction. In an ideal case, this represents a reduction in mass flow in proportion to the chamber pressure which has both near and far field effects. At the exit plane, the reduction in mass flow produces a proportional reduction in density with no change in temperature. Further downstream, where the size of the plume is influenced by ambient pressure, the reduction in mass flow is reflected by a reduction in flow area and other property variations caused by the increase in the ambient-to-chamber pressure ratio. The pressure ratio increase causes a decrease in plume Mach number

and density and an increase in temperature. Ideal gas examples for throttling to 75 percent (expected for the pressure-fed engine) indicate the plume temperature will increase about 5 percent while the flow area will decrease about 20 percent. These changes imply an increase of 20 percent in emissive power and a decrease of 10 percent in plume surface area. If the plume is not opaque, there would also be a reduction resulting from decreased absorption caused by the reduced path lengths through the plume. Considering both near and far field effects of throttling, there is not a clearly significant trend.

Since the emissive power is likely to be influenced primarily by the mixing layer temperatures rather than the interior temperatures, it will be estimated that the radiation variation with throttling will vary approximately with the external area of the plume. Based on the ideal gas example for 75 percent thrust, this can be approximated by varying radiation with the 1/3-power of the thrust level.

As altitude increases, the plume expands and the static temperature and density decrease. The decreased temperature and density tend to decrease the emissive power, while the increase in size tends to compensate by increasing the viewfactors to the plume. If the plume is highly absorptive as a result of particles in the gas, the plume may become opaque near the boundary so that the decrease in density is not significant. In addition, in the altitude range where plume afterburning occurs, the temperature near the boundary will not decrease as significantly as the interior plume temperatures.

Radiation from plume gases reversed into base regions usually have a sudden onset when the flow conditions reach the reverse point, and then the radiation declines as the gas density decreases with increasing altitude. Examples of this behavior on the S-IC and Space Shuttle are shown in Fig. 4.3. In the case of the LRB, the flow reversal radiation is likely to occur in two regions at different times. At low altitude, flow into the LRB base might occur as on the S-IC, while at higher altitudes there may be flow of the reversed gases from the SSME and the LRB plumes into the ET base region. A proper evaluation of these trends will require a detailed study during vehicle development.

For the current preliminary estimate, altitude effects will be handled by two approximations. For the LRB base regions (heat shield, skirt interior, and nozzle exterior), the view of the expanding plume is limited and a behavior dependent on the reversed gases, similar to the S-IC experience, will be used. The variation to be used for these points is given in Fig. 4.4. This represents a slight decrease as the plume expands with altitude until reversal occurs, and then requires an increase of up to twice the sea-level rate. However, the increases is limited to a maximum of 30 Btu/sq-ft-sec, because rates significantly higher than this are considered unlikely based on the conditions represented and past experience.

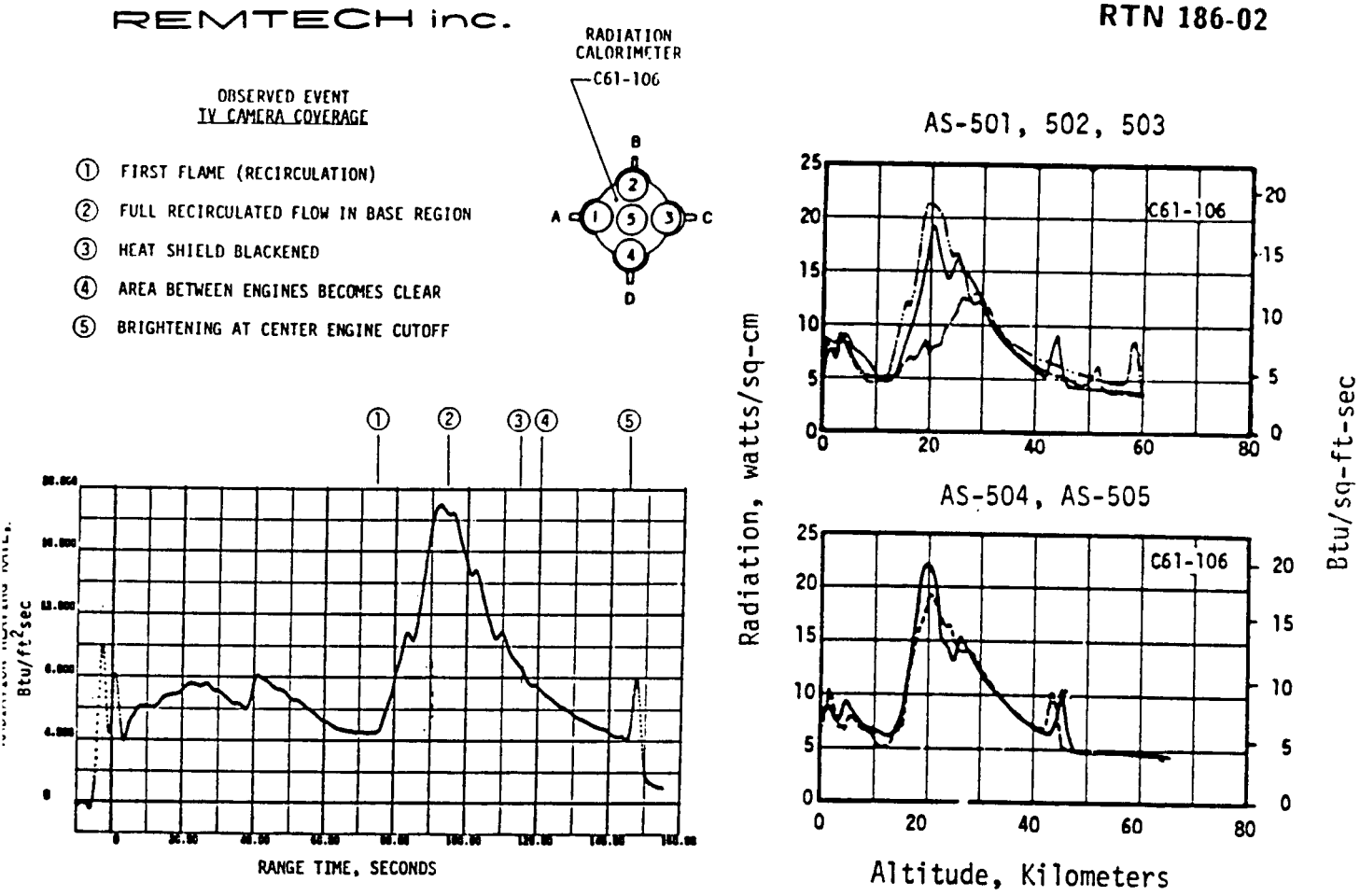

(a) Saturn S-IC data from radiation calorimeter C61-106

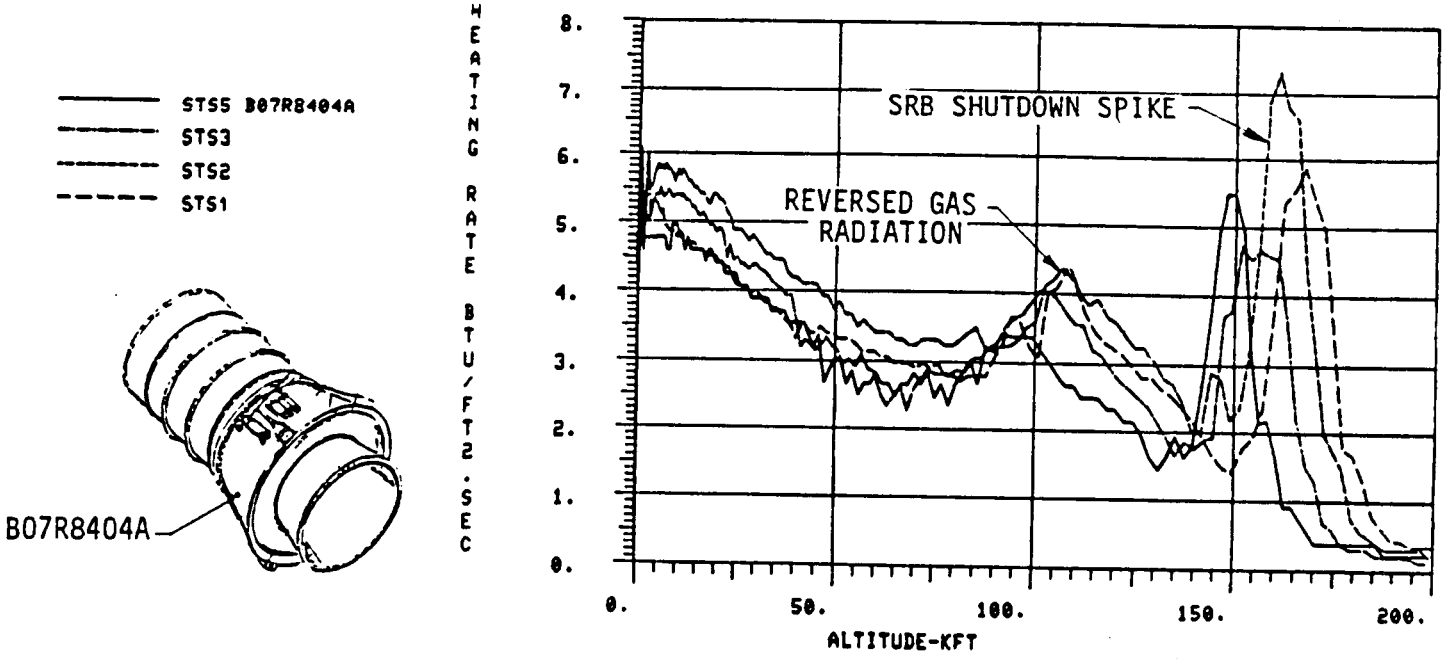

(b) Space Shuttle data from right SRB radiometer B07R8404A

Fig. 4.3 Reversed gas effects on plume radiation

ALTITUDE ADJUSTMENT PROCEDURE:

1. Use adjustment ratios in the figure below for base regions A, B, C, and D in Fig. 4.1.
2. Limit the altitude adjusted rate to 30 Btu/sq-ft-sec.
3. For base regions E and F in Fig. 4.1 use the sea-level rates for all altitudes.

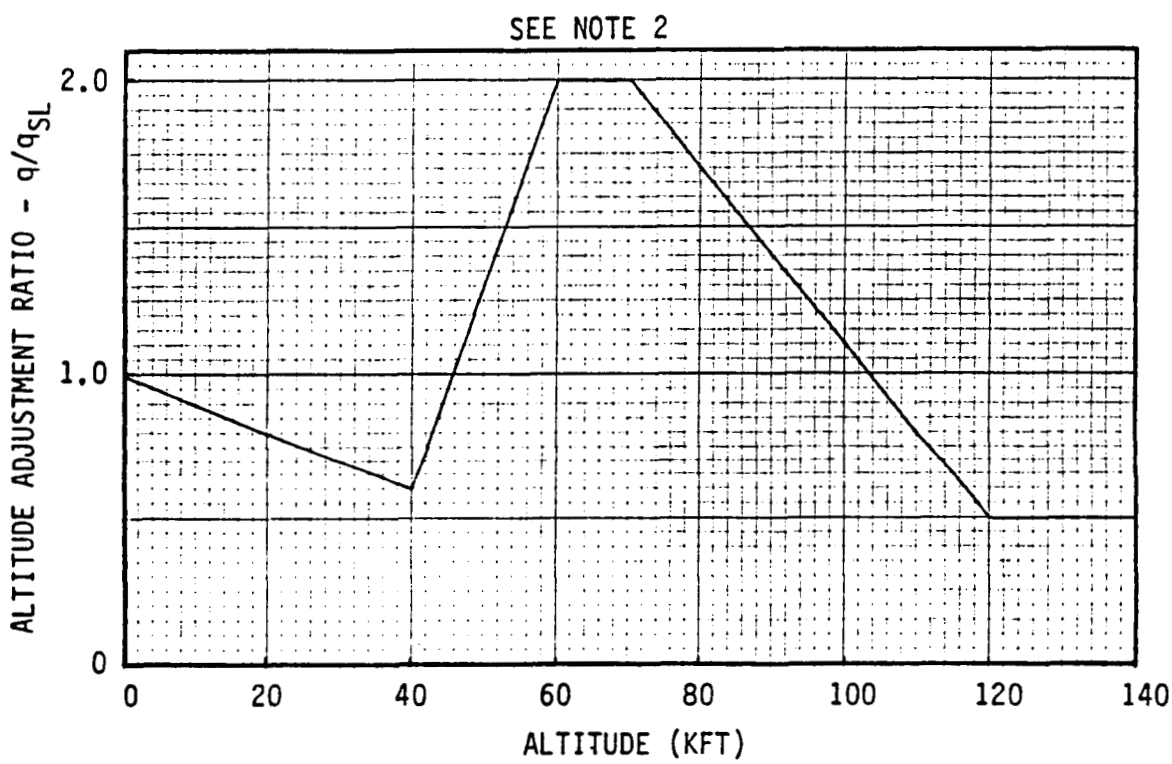

Fig. 4.4 Altitude adjustment procedure for LRB plume radiation.

For points outside the LRB base region (LRB skirt exterior, ET, and Orbiter), reversed gas effects are expected to be less severe. Characteristics of the LRB plume are likely to reduce the severity of the interaction with the SSME plumes which influences the reversal into the ET base region. Altitude effects because of the LRB plumes in these regions will also be small. Because points in these regions have a good view of the entire LRB plumes, the decrease in plume density with altitude is offset by an increase in the plume size. Since it is anticipated that altitude and reversed gas effects will be minor, radiation to these points will be taken to be constant at the sea-level value. This diminishes the peak rates, but does not change the load significantly when compared with the other regions.

The plume model and altitude variation used for the SSME plumes are the data which are used for Space Shuttle predictions [3]. The model and altitude variation are described in Figs. 4.5 and 4.6. The altitude letter codes are usually selected on an area basis by making predictions at representative locations using a band-model code [4] with altitude predictions of the plume gas properties. In this analysis, the SSME altitude codes on the LRB were estimated from similar locations on the SRB.

Sea-level radiation rates and SSME altitude adjustment letter codes for the LRB regions and the representative ET point at the center of the base dome (Body Point 8000) are given in Table 4.1. The rates are moderate except on the nozzle. These rates at the exit plane will diminish rapidly with distance forward of the exit, but heating at the exit is usually the most critical.

The Pressure-Fed LRB generally has higher rates than the Pump-Fed LRB. The higher rates are generally caused by the larger Pressure-Fed plumes and the hotter initial plume cylinder. In addition, the aft portion of the skirt is a cylinder which has a better view of the opposite LRB than the cone of the Pump-Fed LRB. Rates to the forward skirt on the Pressure-Fed stage are lower because the high cone angle reduces the view of both the SSME and LRB plumes. Radiation from exhaust gases of the gas generator used to heat the tank pressurant has not been predicted because there is insufficient information about the design, but it is not expected to be a major radiation source. Assuming the exhaust is dumped from a mast at the outboard trailing edge of the skirt, the primary effect will be on the LRB heat shield surfaces and nozzles. It is not expected to have a significant influence on the high heat shield rates, but the nozzle exterior (Region C2) of the outboard engine (only) should be designed to the same rate as the interior (Region C1). Depending upon the design of the mast, there will be a degree of local heating over a portion of the outboard aft skirt (Region E2), but local thermal protection for this source will cause a minor weight impact.

LRB rates to the ET base at sea level are higher than the SRB, but the altitude

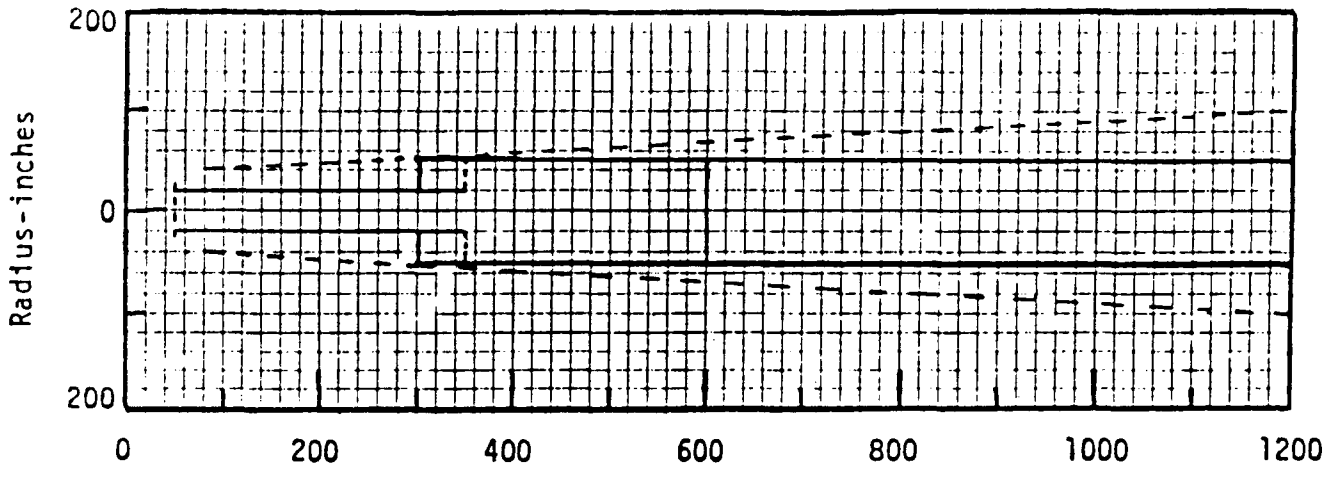

Shape	Emissive power Btu/ft^2-sec	Distance from exit inches	Radius inches
Disk 1 - Transparent	150	50	25
2 - Transparent	120	350	20-50
Cylinder 1 - Opaque	60	50-350	20
2 - Opaque	60	300-600	50
3 - Opaque	40	600-1200	50
Cone - Transparent	12	120-1200	40-100

Fig. 4.5 SSME sea-level plume radiation model (Ref. 2)

Altitude Adjustments for 160 kft							
Code Letter	K	L	M	N	O	P	Q
q_{160k}/q_{SL}	0.06	0.12	0.18	0.24	0.30	-	-
q_{160k}(Btu/ft^2-sec)	-	-	-	-		0.1	0.2

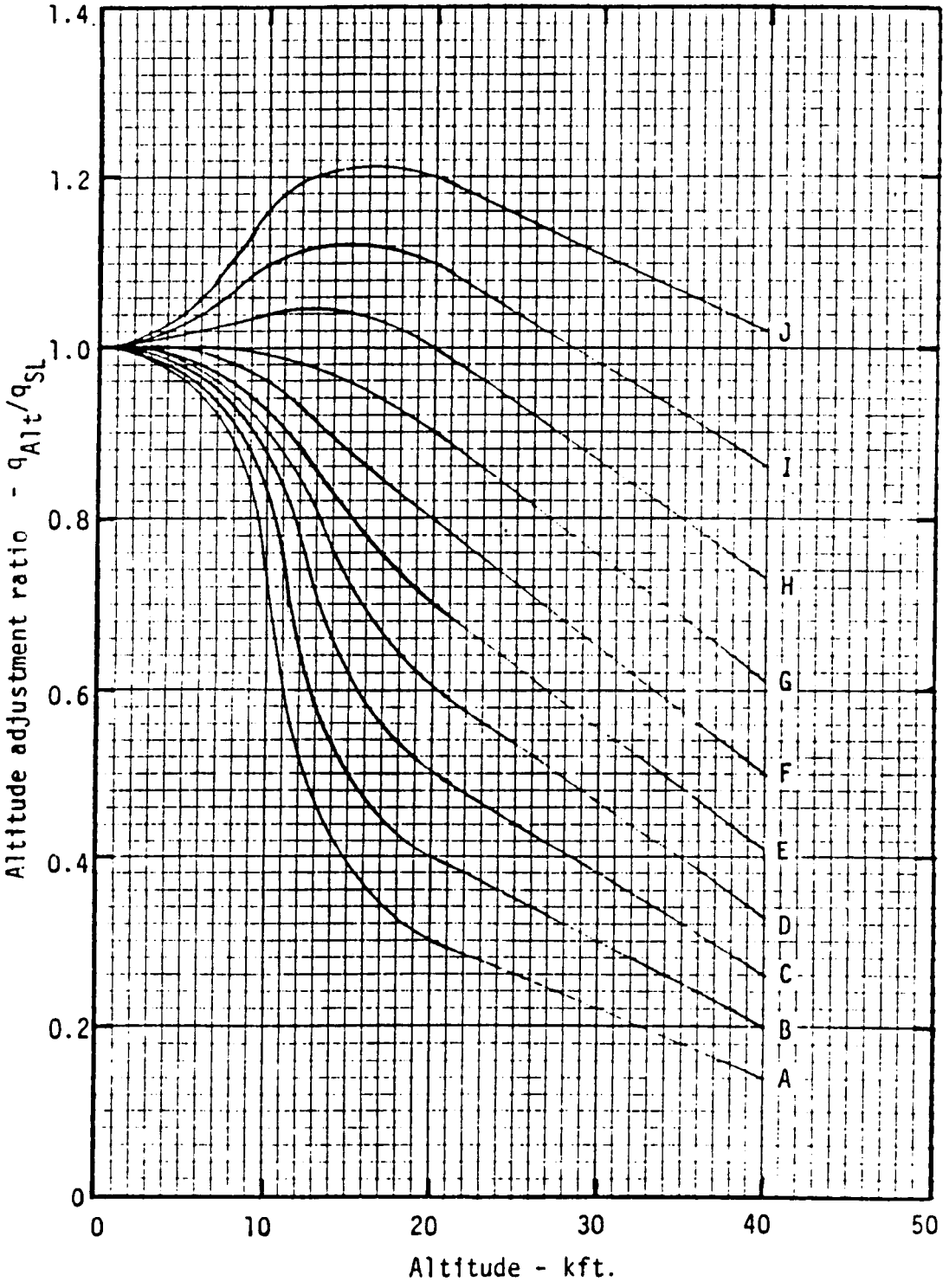

NOTE: Use linear variation with altitude from 40 to 160 kft and constant above 160 kft.

Fig. 4.6 Altitude adjustment ratios for the SSME plume radiation (Ref. 2)

REGION OR BODY POINT (REF. FIG. 4.1)	INCIDENT RADIATION RATE (BTU/SQ-FT-SEC)			
	PUMP-FED		PRESSURE-FED	
	SSME(1)	LRB	SSME(1)	LRB
HEAT SHIELD				
A INNER	1.79 FP	4.78	1.49 FP	7.40
B OUTER	0.49 FP	6.21	0.30 FP	8.07
NOZZLE EXTEROR				
C1 INBOARD	0.0	16.0	0.0	27.3
C2 OUTBOARD	2.86 EP	13.5	6.13 DP	19.5(2)
SKIRT				
D INTERIOR	0.87 EP	6.43	0.91 EP	8.57
AFT SKIRT				
E1 INBOARD	1.67 CN	8.01	2.32 CN	12.1
E2 OUTBOARD	4.04 CP	0.0	4.84 CP	0.0
FORWARD SKIRT				
F1 INBOARD	1.39 CO	4.74	1.20 CO	3.87
F2 OUTBOARD	3.11 CP	0.0	2.50 CP	0.0
ET BASE (3)				
CENTER (BP 8000)	2.96 EP	4.85	2.96 EP	6.16

NOTES:
1. SSME letter codes for altitude adjustment are described in Fig. 4.6. Altitude adjustments for LRB plume radiation are described in Fig. 4.4.
2. Region C2 of the outboard nozzle only on each Pressure-Fed LRB must be designed to the Region C1 environment to account for effects of the heat exchanger exhaust.
3. The current ET base rates are SSME=2.93 EP and SRB=5.96.

Table 4.1: Sea-level Radiation Rates to the LRB and ET

adjustments are likely to result in similar overall loads for the Pump-Fed stage.

Radiation rates for both the SSME and LRB plumes as a function of time and altitude are provided in Tables 4.2 through 4.6. Tables 4.2 and 4.4 are for the LRB base regions, Tables 4.3 and 4.5 are for the exterior regions of the LRB skirt, and Table 4.6 is for the ET base center. These tables include the radiation rates from each propulsion system with the appropriate adjustments for altitude and thrust according to the trajectory and throttle schedules in Section 1. The tables also include the total rate from all plumes and the integrated incident radiation load.

4.3 Convection

Plume induced convective base heating predictions are not generated by a rigorous analytical procedure utilizing a computer code solution, but rely upon judicious scaling of applicable model and flight data. For the two base configurations considered, the classic four engine square arrangement suggested for the LRB is ideally suited for the data base applications since this configuration has been extensively tested and analyzed. Another fortuitous choice in terms of data base applicability was the use of LOX/RP-1 engines up to the 1000 psia range where extensive data also exist.

The model data base was generated in the late 1950's and 1960's; primarily in support of the Saturn I, IB, and V flight programs. These data are reported in Ref. [5] through [10]. Of particular interest are the test reported by Goethert in Ref. [5] and those conducted by Musial and Ward in Ref. [8]. Flight data from LOX/RP-1 stages were extracted from the Saturn I and V flight data reported and summarized in Ref. [1] and [11]. These flight data were generated for chamber pressure conditions and similar trajectories as that proposed for the STS with LRB. Detailed plumes at various altitudes were not determined for the LRB engines; however, nozzle lip pressures and Prandtl-Meyer expansion conditions at various altitudes were estimated from compressible flow tables. Subtle adjustments in the base flow patterns due to gimbaling were not accounted for in this study. The effect of turbine exhaust disposal in the pump-fed nozzle was accounted for in the base gas temperature estimate.

Throttling the engines has a dramatic effect on the convective heating predictions which are a strong function of the nozzle lip to free-stream pressure ratio. The chamber pressure histories provided in Fig. 1.3 and 1.4 were followed in estimating plume interactions, reverse flow conditions, and the onset of free-stream flow separation.

Although convective cooling would probably occur early in flight over base re-

Table 4.2: Pump-Fed LRB Radiation to the LRB Base

			BASE INNER - ZONE A				BASE OUTER - ZONE B			
TIME	ALT	THROTTLE	RADIATION(BTU/SQ-FT-SEC)				RADIATION(BTU/SQ-FT-SEC)			
(SEC)	(FT)	(%)	TOTAL		SSME	LRB	TOTAL		SSME	LRB
			RATE	LOAD	RATE	RATE	RATE	LOAD	RATE	RATE
0.00	95.	75.	6.57	0.	1.79	4.78	6.69	0.	0.49	6.20
10.00	537.	75.	6.54	66.	1.79	4.75	6.67	67.	0.49	6.18
20.00	2080.	75.	6.47	131.	1.79	4.68	6.57	133.	0.49	6.08
30.00	4920.	75.	6.33	195.	1.79	4.54	6.39	198.	0.49	5.90
40.00	9218.	75.	6.07	257.	1.73	4.34	6.11	260.	0.47	5.64
50.00	15188.	75.	5.62	315.	1.56	4.05	5.69	319.	0.43	5.27
60.00	23056.	68.	4.92	368.	1.35	3.57	5.00	373.	0.37	4.63
65.00	27677.	65.	4.52	391.	1.23	3.30	4.62	397.	0.34	4.28
70.00	32728.	68.	4.19	413.	1.09	3.10	4.33	419.	0.30	4.03
76.20	40000.	71.	3.71	438.	0.89	2.81	3.90	445.	0.25	3.65
80.00	44439.	73.	5.17	455.	0.87	4.30	5.83	463.	0.24	5.59
85.00	51272.	75.	7.46	486.	0.82	6.64	8.86	500.	0.23	8.63
90.00	58804.	75.	9.93	530.	0.77	9.16	12.12	552.	0.22	11.90
90.70	60000.	75.	10.32	537.	0.76	9.56	12.64	561.	0.22	12.42
96.60	70000.	75.	10.26	597.	0.70	9.56	12.63	636.	0.21	12.42
100.00	75818.	75.	9.38	631.	0.66	8.73	11.54	677.	0.20	11.34
103.00	81665.	75.	8.51	658.	0.62	7.89	10.44	710.	0.19	10.25
110.00	95308.	70.	6.33	709.	0.53	5.80	7.71	773.	0.18	7.53
120.00	117102.	63.	3.03	756.	0.38	2.65	3.59	830.	0.15	3.44
130.00	140926.	56.	2.40	783.	0.23	2.17	2.94	862.	0.12	2.82
131.50	144620.	55.	2.36	787.	0.20	2.16	2.92	867.	0.12	2.80

			NOZZLE INBD - ZONE C1				NOZZLE OUTBD - ZONE C2			
TIME	ALT	THROTTLE	RADIATION(BTU/SQ-FT-SEC)				RADIATION(BTU/SQ-FT-SEC)			
(SEC)	(FT)	(%)	TOTAL		SSME	LRB	TOTAL		SSME	LRB
			RATE	LOAD	RATE	RATE	RATE	LOAD	RATE	RATE
0.00	95.	75.	16.01	0.	0.00	16.01	16.35	0.	2.86	13.49
10.00	537.	75.	15.94	160.	0.00	15.94	16.28	163.	2.86	13.43
20.00	2080.	75.	15.70	318.	0.00	15.70	16.06	325.	2.85	13.22
30.00	4920.	75.	15.24	473.	0.00	15.24	15.65	483.	2.82	12.84
40.00	9218.	75.	14.55	622.	0.00	14.55	14.95	636.	2.69	12.26
50.00	15188.	75.	13.60	762.	0.00	13.60	13.74	780.	2.29	11.45
60.00	23056.	68.	11.96	890.	0.00	11.96	11.95	908.	1.88	10.07
65.00	27677.	65.	11.05	948.	0.00	11.05	10.99	966.	1.68	9.31
70.00	32728.	68.	10.41	1001.	0.00	10.41	10.24	1019.	1.47	8.77
76.20	40000.	71.	9.43	1063.	0.00	9.43	9.11	1079.	1.17	7.94
80.00	44439.	73.	14.43	1108.	0.00	14.43	13.29	1121.	1.13	12.16
85.00	51272.	75.	22.27	1200.	0.00	22.27	19.82	1204.	1.07	18.75
90.00	58804.	75.	30.00	1331.	0.00	30.00	26.87	1321.	1.00	25.87
90.70	60000.	75.	30.00	1352.	0.00	30.00	27.99	1340.	0.99	27.00
96.60	70000.	75.	30.00	1529.	0.00	30.00	27.90	1505.	0.90	27.00
100.00	75818.	75.	29.26	1629.	0.00	29.26	25.50	1596.	0.85	24.64
103.00	81665.	75.	26.45	1713.	0.00	26.45	23.08	1669.	0.80	22.28
110.00	95308.	70.	19.44	1874.	0.00	19.44	17.05	1809.	0.68	16.38
120.00	117102.	63.	8.88	2015.	0.00	8.88	7.96	1934.	0.48	7.48
130.00	140926.	56.	7.27	2096.	0.00	7.27	6.40	2006.	0.27	6.13
131.50	144620.	55.	7.23	2107.	0.00	7.23	6.32	2015.	0.24	6.09

TABLE 4.2 (CONCLUDED)

PUMP-FED LRB PLUME RADIATION TO THE LRB BASE

			SKIRT INNER LIP - ZONE D			
TIME	ALT	THROTTLE	RADIATION(BTU/SQ-FT-SEC)			
(SEC)	(FT)	(%)	TOTAL		SSME	LRB
			RATE	LOAD	RATE	RATE
0.00	95.	75.	7.29	0.	0.87	6.42
10.00	537.	75.	7.26	73.	0.87	6.40
20.00	2080.	75.	7.16	145.	0.87	6.30
30.00	4920.	75.	6.97	216.	0.86	6.11
40.00	9218.	75.	6.66	284.	0.82	5.84
50.00	15188.	75.	6.15	348.	0.70	5.45
60.00	23056.	68.	5.37	405.	0.57	4.80
65.00	27677.	65.	4.95	431.	0.51	4.43
70.00	32728.	68.	4.62	455.	0.45	4.18
76.20	40000.	71.	4.14	482.	0.36	3.78
80.00	44439.	73.	6.14	502.	0.35	5.79
85.00	51272.	75.	9.26	540.	0.33	8.93
90.00	58804.	75.	12.64	595.	0.32	12.32
90.70	60000.	75.	13.17	604.	0.31	12.86
96.60	70000.	75.	13.15	682.	0.29	12.86
100.00	75818.	75.	12.02	724.	0.28	11.74
103.00	81665.	75.	10.88	759.	0.27	10.61
110.00	95308.	70.	8.04	825.	0.24	7.80
120.00	117102.	63.	3.75	884.	0.19	3.56
130.00	140926.	56.	3.06	918.	0.14	2.92
131.50	144620.	55.	3.03	923.	0.13	2.90

Table 4.3: Pump-Fed LRB Radiation to the LRB Exterior

TIME (SEC)	ALT (FT)	THROTTLE (%)	SKIRT AFT INBD - ZONE E1 RADIATION(BTU/SQ-FT-SEC) TOTAL RATE	TOTAL LOAD	SSME RATE	LRB RATE	SKIRT AFT OUTBD - ZONE E2 RADIATION(BTU/SQ-FT-SEC) TOTAL RATE	TOTAL LOAD	SSME RATE	LRB RATE
0.00	95.	75.	9.68	0.	1.67	8.01	4.04	0.	4.04	0.00
10.00	537.	75.	9.68	97.	1.67	8.01	4.03	40.	4.03	0.00
20.00	2080.	75.	9.67	194.	1.66	8.01	4.02	81.	4.02	0.00
30.00	4920.	75.	9.65	290.	1.64	8.01	3.96	121.	3.96	0.00
40.00	9218.	75.	9.51	386.	1.50	8.01	3.63	159.	3.63	0.00
50.00	15188.	75.	9.04	479.	1.03	8.01	2.50	189.	2.50	0.00
60.00	23056.	68.	8.54	567.	0.77	7.77	1.87	211.	1.87	0.00
65.00	27677.	65.	8.32	609.	0.68	7.64	1.65	220.	1.65	0.00
70.00	32728.	68.	8.31	650.	0.58	7.73	1.40	227.	1.40	0.00
76.20	40000.	71.	8.28	702.	0.43	7.85	1.05	235.	1.05	0.00
80.00	44439.	73.	8.35	733.	0.43	7.92	1.02	239.	1.02	0.00
85.00	51272.	75.	8.44	775.	0.43	8.01	0.96	244.	0.96	0.00
90.00	58804.	75.	8.44	818.	0.43	8.01	0.90	249.	0.90	0.00
90.70	60000.	75.	8.44	823.	0.43	8.01	0.89	249.	0.89	0.00
96.60	70000.	75.	8.44	873.	0.43	8.01	0.81	254.	0.81	0.00
100.00	75818.	75.	8.43	902.	0.42	8.01	0.77	257.	0.77	0.00
103.00	81665.	75.	8.43	927.	0.42	8.01	0.72	259.	0.72	0.00
110.00	95308.	70.	8.25	986.	0.42	7.83	0.61	264.	0.61	0.00
120.00	117102.	63.	7.97	1067.	0.41	7.56	0.44	269.	0.44	0.00
130.00	140926.	56.	7.68	1145.	0.41	7.27	0.25	273.	0.25	0.00
131.50	144620.	55.	7.63	1156.	0.41	7.22	0.22	273.	0.22	0.00

TIME (SEC)	ALT (FT)	THROTTLE (%)	SKIRT FWD INBD - ZONE F1 RADIATION(BTU/SQ-FT-SEC) TOTAL RATE	TOTAL LOAD	SSME RATE	LRB RATE	SKIRT FWD OUTBD - ZONE F2 RADIATION(BTU/SQ-FT-SEC) TOTAL RATE	TOTAL LOAD	SSME RATE	LRB RATE
0.00	95.	75.	6.13	0.	1.39	4.74	3.11	0.	3.11	0.00
10.00	537.	75.	6.13	61.	1.39	4.74	3.11	31.	3.11	0.00
20.00	2080.	75.	6.12	123.	1.38	4.74	3.09	62.	3.09	0.00
30.00	4920.	75.	6.10	184.	1.36	4.74	3.05	93.	3.05	0.00
40.00	9218.	75.	5.99	244.	1.25	4.74	2.80	122.	2.80	0.00
50.00	15188.	75.	5.60	302.	0.86	4.74	1.92	146.	1.92	0.00
60.00	23056.	68.	5.24	356.	0.64	4.60	1.44	162.	1.44	0.00
65.00	27677.	65.	5.09	382.	0.57	4.52	1.27	169.	1.27	0.00
70.00	32728.	68.	5.06	407.	0.48	4.58	1.08	175.	1.08	0.00
76.20	40000.	71.	5.01	439.	0.36	4.65	0.81	181.	0.81	0.00
80.00	44439.	73.	5.05	458.	0.36	4.69	0.78	184.	0.78	0.00
85.00	51272.	75.	5.11	483.	0.37	4.74	0.74	188.	0.74	0.00
90.00	58804.	75.	5.11	509.	0.37	4.74	0.70	191.	0.70	0.00
90.70	60000.	75.	5.11	512.	0.37	4.74	0.69	192.	0.69	0.00
96.60	70000.	75.	5.12	542.	0.38	4.74	0.63	196.	0.63	0.00
100.00	75818.	75.	5.12	560.	0.38	4.74	0.60	198.	0.60	0.00
103.00	81665.	75.	5.12	575.	0.38	4.74	0.56	200.	0.56	0.00
110.00	95308.	70.	5.02	611.	0.39	4.63	0.48	203.	0.48	0.00
120.00	117102.	63.	4.87	660.	0.40	4.47	0.35	207.	0.35	0.00
130.00	140926.	56.	4.71	708.	0.41	4.30	0.21	210.	0.21	0.00
131.50	144620.	55.	4.68	715.	0.41	4.27	0.19	211.	0.19	0.00

Table 4.4: Pressure-Fed LRB Radiation to the LRB Base

TIME (SEC)	ALT (FT)	THROTTLE (%)	BASE INNER - ZONE A RADIATION(BTU/SQ-FT-SEC) TOTAL RATE	TOTAL LOAD	SSME RATE	LRB RATE	BASE OUTER - ZONE B RADIATION(BTU/SQ-FT-SEC) TOTAL RATE	TOTAL LOAD	SSME RATE	LRB RATE
0.00	0.	100.	8.89	0.	1.49	7.40	8.37	0.	0.30	8.07
10.00	988.	100.	8.82	89.	1.49	7.33	8.29	83.	0.30	7.99
20.00	3954.	100.	8.60	176.	1.49	7.11	8.05	165.	0.30	7.75
30.00	9072.	100.	8.17	259.	1.44	6.73	7.63	243.	0.29	7.34
30.01	9073.	75.	7.56	260.	1.44	6.11	6.96	243.	0.29	6.67
40.00	16092.	75.	6.92	332.	1.28	5.64	6.41	310.	0.26	6.15
50.00	24713.	75.	6.15	397.	1.09	5.06	5.74	371.	0.22	5.52
60.00	35229.	75.	5.21	454.	0.85	4.35	4.92	424.	0.17	4.75
63.90	40000.	75.	4.78	473.	0.75	4.03	4.55	443.	0.15	4.40
65.00	41319.	75.	5.39	479.	0.74	4.65	5.23	448.	0.15	5.08
70.00	48042.	75.	8.52	514.	0.70	7.82	8.67	483.	0.15	8.53
75.00	55422.	75.	11.95	565.	0.66	11.29	12.46	536.	0.14	12.31
77.80	60000.	75.	14.08	601.	0.64	13.45	14.81	574.	0.14	14.66
80.00	63460.	75.	14.07	632.	0.62	13.45	14.80	606.	0.14	14.66
85.00	72139.	75.	13.59	702.	0.57	13.02	14.33	679.	0.14	14.19
90.00	81442.	75.	11.66	765.	0.52	11.14	12.28	746.	0.13	12.15
100.00	101970.	75.	7.41	860.	0.41	7.00	7.76	846.	0.12	7.63
108.00	120526.	75.	3.67	904.	0.31	3.36	3.78	892.	0.12	3.67
110.00	125165.	73.	3.62	912.	0.29	3.33	3.75	900.	0.11	3.63
119.80	150414.	65.	3.36	946.	0.15	3.21	3.60	936.	0.10	3.50

TIME (SEC)	ALT (FT)	THROTTLE (%)	NOZZLE INBOARD - ZONE C1 RADIATION(BTU/SQ-FT-SEC) TOTAL RATE	TOTAL LOAD	SSME RATE	LRB RATE	NOZZLE OUTBOARD - ZONE C2 RADIATION(BTU/SQ-FT-SEC) TOTAL RATE	TOTAL LOAD	SSME RATE	LRB RATE
0.00	0.	100.	27.30	0.	0.00	27.30	25.63	0.	6.13	19.50
10.00	988.	100.	27.03	272.	0.00	27.03	25.42	255.	6.11	19.31
20.00	3954.	100.	26.22	538.	0.00	26.22	24.80	506.	6.07	18.73
30.00	9072.	100.	24.82	793.	0.00	24.82	23.36	747.	5.63	17.73
30.01	9073.	75.	22.55	793.	0.00	22.55	21.74	747.	5.63	16.11
40.00	16092.	75.	20.81	1010.	0.00	20.81	19.08	951.	4.22	14.87
50.00	24713.	75.	18.67	1207.	0.00	18.67	16.63	1130.	3.29	13.34
60.00	35229.	75.	16.07	1381.	0.00	16.07	13.89	1282.	2.42	11.48
63.90	40000.	75.	14.88	1441.	0.00	14.88	12.65	1334.	2.02	10.63
65.00	41319.	75.	17.17	1459.	0.00	17.17	14.27	1349.	2.00	12.27
70.00	48042.	75.	28.85	1574.	0.00	28.85	22.50	1441.	1.89	20.60
75.00	55422.	75.	30.00	1721.	0.00	30.00	31.53	1576.	1.78	29.76
77.80	60000.	75.	30.00	1805.	0.00	30.00	31.70	1665.	1.70	30.00
80.00	63460.	75.	30.00	1871.	0.00	30.00	31.65	1734.	1.65	30.00
85.00	72139.	75.	30.00	2021.	0.00	30.00	31.51	1892.	1.51	30.00
90.00	81442.	75.	30.00	2171.	0.00	30.00	30.71	2048.	1.36	29.35
100.00	101970.	75.	25.82	2450.	0.00	25.82	19.47	2299.	1.03	18.44
108.00	120526.	75.	12.40	2603.	0.00	12.40	9.59	2415.	0.73	8.86
110.00	125165.	73.	12.29	2628.	0.00	12.29	9.44	2434.	0.66	8.78
119.80	150414.	65.	11.82	2746.	0.00	11.82	8.70	2523.	0.25	8.45

TABLE 4.4 (CONCLUDED)

PRESSURE-FED LRB PLUME RADIATION TO THE LRB BASE

			SKIRT INNER LIP - ZONE D			
TIME	ALT	THROTTLE	RADIATION(BTU/SQ-FT-SEC)			
(SEC)	(FT)	(%)	TOTAL		SSME	LRB
			RATE	LOAD	RATE	RATE
0.00	0.	100.	9.48	0.	0.91	8.57
10.00	988.	100.	9.39	94.	0.91	8.49
20.00	3954.	100.	9.13	187.	0.90	8.23
30.00	9072.	100.	8.65	276.	0.86	7.79
30.01	9073.	75.	7.94	276.	0.86	7.08
40.00	16092.	75.	7.24	352.	0.71	6.53
50.00	24713.	75.	6.44	420.	0.57	5.86
60.00	35229.	75.	5.48	480.	0.44	5.04
63.90	40000.	75.	5.04	500.	0.37	4.67
65.00	41319.	75.	5.76	506.	0.37	5.39
70.00	48042.	75.	9.41	544.	0.35	9.06
75.00	55422.	75.	13.42	601.	0.34	13.08
77.80	60000.	75.	15.90	642.	0.33	15.57
80.00	63460.	75.	15.89	677.	0.32	15.57
85.00	72139.	75.	15.37	755.	0.30	15.07
90.00	81442.	75.	13.18	827.	0.28	12.90
100.00	101970.	75.	8.34	934.	0.23	8.10
108.00	120526.	75.	4.08	984.	0.19	3.89
110.00	125165.	73.	4.04	992.	0.18	3.86
119.80	150414.	65.	3.83	1031.	0.12	3.71

Table 4.5: Pressure-Fed LRB Radiation to the LRB Exterior

TIME (SEC)	ALT (FT)	THROTTLE (%)	SKIRT AFT INBD - ZONE E1 RADIATION(BTU/SQ-FT-SEC) TOTAL RATE	TOTAL LOAD	SSME RATE	LRB RATE	SKIRT AFT OUTBD - ZONE E2 RADIATION(BTU/SQ-FT-SEC) TOTAL RATE	TOTAL LOAD	SSME RATE	LRB RATE
0.00	0.	100.	14.42	0.	2.32	12.10	4.84	0.	4.84	0.00
10.00	988.	100.	14.41	144.	2.31	12.10	4.83	48.	4.83	0.00
20.00	3954.	100.	14.40	288.	2.30	12.10	4.79	96.	4.79	0.00
30.00	9072.	100.	14.20	431.	2.10	12.10	4.37	142.	4.37	0.00
30.01	9073.	75.	13.09	431.	2.10	10.99	4.37	142.	4.37	0.00
40.00	16092.	75.	12.36	558.	1.36	10.99	2.85	178.	2.85	0.00
50.00	24713.	75.	12.02	680.	1.03	10.99	2.15	203.	2.15	0.00
60.00	35229.	75.	11.73	799.	0.74	10.99	1.54	222.	1.54	0.00
63.90	40000.	75.	11.60	845.	0.60	10.99	1.26	227.	1.26	0.00
65.00	41319.	75.	11.60	857.	0.60	10.99	1.25	229.	1.25	0.00
70.00	48042.	75.	11.59	915.	0.60	10.99	1.18	235.	1.18	0.00
75.00	55422.	75.	11.59	973.	0.60	10.99	1.11	240.	1.11	0.00
77.80	60000.	75.	11.59	1006.	0.60	10.99	1.07	243.	1.07	0.00
80.00	63460.	75.	11.59	1031.	0.59	10.99	1.03	246.	1.03	0.00
85.00	72139.	75.	11.58	1089.	0.59	10.99	0.95	251.	0.95	0.00
90.00	81442.	75.	11.58	1147.	0.59	10.99	0.86	255.	0.86	0.00
100.00	101970.	75.	11.57	1263.	0.58	10.99	0.66	263.	0.66	0.00
108.00	120526.	75.	11.57	1355.	0.57	10.99	0.48	267.	0.48	0.00
110.00	125165.	73.	11.47	1378.	0.57	10.90	0.44	268.	0.44	0.00
119.80	150414.	65.	11.04	1489.	0.56	10.48	0.19	271.	0.19	0.00

TIME (SEC)	ALT (FT)	THROTTLE (%)	SKIRT FWD INBD - ZONE F1 RADIATION(BTU/SQ-FT-SEC) TOTAL RATE	TOTAL LOAD	SSME RATE	LRB RATE	SKIRT FWD OUTBD - ZONE F2 RADIATION(BTU/SQ-FT-SEC) TOTAL RATE	TOTAL LOAD	SSME RATE	LRB RATE
0.00	0.	100.	5.07	0.	1.20	3.87	2.50	0.	2.50	0.00
10.00	988.	100.	5.07	51.	1.20	3.87	2.49	25.	2.49	0.00
20.00	3954.	100.	5.06	101.	1.19	3.87	2.48	50.	2.48	0.00
30.00	9072.	100.	4.95	151.	1.08	3.87	2.26	73.	2.26	0.00
30.01	9073.	75.	4.60	151.	1.08	3.52	2.26	74.	2.26	0.00
40.00	16092.	75.	4.22	195.	0.71	3.52	1.47	92.	1.47	0.00
50.00	24713.	75.	4.05	237.	0.53	3.52	1.11	105.	1.11	0.00
60.00	35229.	75.	3.90	277.	0.38	3.52	0.79	115.	0.79	0.00
63.90	40000.	75.	3.83	292.	0.31	3.52	0.65	117.	0.65	0.00
65.00	41319.	75.	3.83	296.	0.31	3.52	0.64	118.	0.64	0.00
70.00	48042.	75.	3.83	315.	0.32	3.52	0.61	121.	0.61	0.00
75.00	55422.	75.	3.83	334.	0.32	3.52	0.58	124.	0.58	0.00
77.80	60000.	75.	3.84	345.	0.32	3.52	0.56	126.	0.56	0.00
80.00	63460.	75.	3.84	353.	0.32	3.52	0.54	127.	0.54	0.00
85.00	72139.	75.	3.84	373.	0.32	3.52	0.50	130.	0.50	0.00
90.00	81442.	75.	3.84	392.	0.33	3.52	0.46	132.	0.46	0.00
100.00	101970.	75.	3.85	430.	0.34	3.52	0.37	136.	0.37	0.00
108.00	120526.	75.	3.86	461.	0.34	3.52	0.28	139.	0.28	0.00
110.00	125165.	73.	3.83	469.	0.35	3.48	0.26	139.	0.26	0.00
119.80	150414.	65.	3.71	506.	0.36	3.35	0.14	141.	0.14	0.00

TABLE 4.6

LRB PLUME RADIATION TO THE ET BASE (BP 8000)

PUMP-FED LRB

TIME (SEC)	ALT (FT)	THROTTLE (%)	RADIATION(BTU/SQ-FT-SEC) TOTAL RATE	TOTAL LOAD	SSME RATE	LRB RATE
0.00	95.	75.	7.81	0.	2.96	4.85
10.00	537.	75.	7.81	78.	2.96	4.85
20.00	2080.	75.	7.79	156.	2.94	4.85
30.00	4920.	75.	7.77	234.	2.92	4.85
40.00	9218.	75.	7.64	311.	2.79	4.85
50.00	15188.	75.	7.22	385.	2.37	4.85
60.00	23056.	68.	6.64	454.	1.94	4.70
65.00	27677.	65.	6.37	487.	1.74	4.62
70.00	32728.	68.	6.21	518.	1.53	4.68
76.20	40000.	71.	5.97	556.	1.21	4.75
80.00	44439.	73.	5.97	579.	1.17	4.80
85.00	51272.	75.	5.96	609.	1.11	4.85
90.00	58804.	75.	5.89	638.	1.04	4.85
90.70	60000.	75.	5.88	642.	1.03	4.85
96.60	70000.	75.	5.79	677.	0.94	4.85
100.00	75818.	75.	5.73	696.	0.88	4.85
103.00	81665.	75.	5.68	714.	0.83	4.85
110.00	95308.	70.	5.44	752.	0.70	4.74
120.00	117102.	63.	5.08	805.	0.50	4.58
130.00	140926.	56.	4.68	854.	0.28	4.40
131.50	144620.	55.	4.62	861.	0.24	4.37

PRESSURE-FED LRB

TIME (SEC)	ALT (FT)	THROTTLE (%)	RADIATION(BTU/SQ-FT-SEC) TOTAL RATE	TOTAL LOAD	SSME RATE	LRB RATE
0.00	0.	100.	9.12	0.	2.96	6.16
10.00	988.	100.	9.11	91.	2.95	6.16
20.00	3954.	100.	9.09	182.	2.93	6.16
30.00	9072.	100.	8.95	272.	2.79	6.16
30.01	9073.	75.	8.39	272.	2.79	5.60
40.00	16092.	75.	7.90	354.	2.30	5.60
50.00	24713.	75.	7.47	431.	1.87	5.60
60.00	35229.	75.	7.02	503.	1.42	5.60
63.90	40000.	75.	6.81	530.	1.21	5.60
65.00	41319.	75.	6.80	538.	1.20	5.60
70.00	48042.	75.	6.74	571.	1.14	5.60
75.00	55422.	75.	6.67	605.	1.07	5.60
77.80	60000.	75.	6.62	624.	1.03	5.60
80.00	63460.	75.	6.59	638.	1.00	5.60
85.00	72139.	75.	6.51	671.	0.92	5.60
90.00	81442.	75.	6.43	703.	0.83	5.60
100.00	101970.	75.	6.24	766.	0.64	5.60
108.00	120526.	75.	6.06	816.	0.47	5.60
110.00	125165.	73.	5.97	828.	0.42	5.55
119.80	150414.	65.	5.53	884.	0.19	5.34

gion surfaces heated by radiation, a conservative approach is to specific zero convection until the onset of recirculation. The altitude of incipient recirculation was estimated to be approximately 36,000 feet for both the pump-fed and pressure-fed configurations; the differences in engine spacing and chamber pressure compensate to provide very similar plume interactions. Because of trajectory differences, this altitude corresponds to 60 seconds for the pressure-fed LRB and 73 seconds for the pump-fed LRB.

Maximum recirculation or choked flow for the recirculated gases which escape from the base is predicted from Ref. [5] to occur at 75,000 feet or 87 seconds for the pressure-fed LRB and 99 seconds for the pump-fed LRB. Convective heating within the base cluster will remain constant with time after 87 seconds for the pressure-fed concept which maintains 600 psia chamber pressure. A linear decline in chamber pressure from 1033 to 715 over the last 28 seconds of pump-fed first stage ascent will produce a corresponding decline in convective heating.

An exact prediction of the base gas recovery temperature would require detailed nozzle boundary layer calculations adjusted for wall temperature effects and turbine exhaust mixing (in the case of the pump-fed LRB). In lieu of this level of detail, a procedure based upon Ref. [10] predicts the choked level of base gas temperature as a function of chamber temperature and nozzle exit Reynolds number. For the pressure-fed LRB, the gas temperature is predicted to be approximately 3000°R for the choked condition. With turbine exhaust mixing the pump-fed temperature is about 300° cooler or 2700°R. Thrust reduction for the pump-fed LRB was accounted for in the heat transfer coefficient; gas temperature was assumed to be unaffected.

The convective heating predictions for the generic zones shown in Fig. 4.1 are listed in Tables 4.7 through 4.10. Tables 4.7 and 4.8 display the environments for the engines and base heat shield respectively. Engine zone C1 and base heat shield zone A heating levels were based upon Saturn I and Saturn V flight data normalized to chamber pressure to the 0.8 power; then displayed versus area ratio. In general, convective heating due to reverse plume gases increases with chamber pressure, decreases with nozzle expansion ratio, and decreases as the distance between nozzles increases. Accounting for these effects resulting in peak heating near the nozzle exit plane in the low teens for a cold nozzle surface. Model data trends show a significant amplification in the convective heating due to the skirt. This trend would be particularly applicable to the LRB configurations which have close engine spacing and a "tight" skirt surrounding the engines. The final levels of convective heating are relatively severe as displayed in Table 4.7 for the engine nozzle inboard surfaces near the exit plane.

Heating decreases as the flow into the base cools, diffuses, and turns as it

PUMP-FED

Flight Time (Seconds)	T_{rec} (°R)	Inboard Zone C1		Outboard Zone C2	
		h_c	q_c	h_c	q_c
0	560	0	0	0	0
72	595	0	0	0	0
73	600	0.00017	0.01	0.00017	0.01
76.2	900	0.00694	2.5	0.00139	0.50
80	1190	0.00754	4.9	0.00162	1.05
85	1600	0.00791	8.38	0.00175	1.85
90	2000	0.00815	11.90	0.00178	2.60
90.7	2050	0.00825	12.46	0.00180	2.72
96.6	2530	0.00832	16.55	0.00183	3.65
99	2721	0.00832	18.15	0.00184	4.01
100		0.00832	18.15	0.00184	4.01
103		0.00832	18.15	0.00184	4.01
110		0.00779	17.0	0.00173	3.77
120		0.00708	15.45	0.00156	3.40
130	↓	0.00637	13.90	0.00138	3.0
131.5	2721	0.00626	13.65	0.00135	2.95

PRESSURE-FED

Flight Time (Seconds)	T_{rec} (°R)	Inboard Zone C1		Outboard Zone C2	
		h_c	q_c	h_c	q_c
0	560	0	0	0	0
59	585	0	0	0	0
60	590	0.00020	0.01	0.00020	0.01
63.9	950	0.00500	2.05	0.00109	0.45
65	1060	0.00519	2.7	0.00106	0.55
70	1490	0.00568	5.4	0.00111	1.05
75	1935	0.00595	8.3	0.00116	1.62
77.8	2160	0.00611	9.9	0.00114	1.85
80	2370	0.00596	10.9	0.00116	2.12
85	2800	0.00611	13.8	0.00112	2.65
87	2930	0.00626	14.95	0.00119	2.85
90					
98					
100					
108					
110	↓	↓	↓	↓	↓
119.8	2930	0.00626	14.95	0.00119	2.84

Table 4.7: Convective Base Heating – Engine Nozzles

PUMP-FED

Flight Time (Seconds)	T_{rec} (°R)	Inner Region A		Outer Zone B	
		h_c	q_c	h_c	q_c
0	560	0	0	0	0
72	595	0	0	0	0
73	600	0.00017	0.01	0.00017	0.01
76.2	900	0.00122	0.44	0.00047	0.17
80	1190	0.00140	0.91	0.00052	0.34
85	1600	0.00147	1.56	0.00057	0.60
90	2000	0.00155	2.26	0.00058	0.85
90.7	2050	0.00157	2.37	0.00060	0.90
96.6	2530	0.00159	3.16	0.00059	1.18
99	2721	0.00158	3.45	0.00061	1.31
100		0.00158	3.45	0.00061	1.31
103		0.00158	3.45	0.00061	1.31
110		0.00148	3.22	0.00056	1.23
120		0.00134	2.93	0.00050	1.10
130	↓	0.00120	2.62	0.00045	0.99
131.5	2721	0.00118	2.57	0.00044	0.97

PRESSURE-FED

Flight Time (Seconds)	T_{rec} (°R)	Inner Zone A		Outer Zone B	
		h_c	q_c	h_c	q_c
0	560	0	0	0	0
59	585	0	0	0	0
60	590	0.00020	0.01	0.00020	0.01
63.9	950	0.00090	0.37	0.00029	0.12
65	1060	0.00086	0.45	0.00031	0.16
70	1490	0.00094	0.89	0.00035	0.33
75	1935	0.00096	1.34	0.00037	0.51
77.8	2160	0.00098	1.59	0.00036	0.59
80	2370	0.00098	1.79	0.00037	0.67
85	2800	0.00098	2.22	0.00038	0.85
87	2930	0.00099	2.38	0.00038	0.91
90					
98					
100					
108					
110	↓	↓	↓	↓	↓
119.8	2930	0.00099	2.38	0.00038	0.91

Table 4.8: Convective Base Heating – Base Heat Shield

PUMP-FED

Flight Time (Seconds)	T_{rec} (°R)	Zone D	
		h_c	q_c
0	560	0	0
72	595	0	0
73	600	0.00017	0.01
76.2	900	0.00278	1.0
80	1190	0.00331	2.15
85	1600	0.00335	3.55
90	2000	0.00346	5.05
90.7	2050	0.00348	5.25
96.6	2530	0.00352	7.0
99	2721	0.00351	7.65
100		0.00351	7.65
103		0.00351	7.65
110		0.00328	7.15
120		0.00298	6.50
130	↓	0.00266	5.80
131.5	2721	0.00261	5.70

PRESSURE-FED

Flight Time (Seconds)	T_{rec} (°R)	Zone D	
		h_c	q_c
	560	0	0
59	585	0	0
60	590	0.00020	0.01
63.9	950	0.00176	0.72
65	1060	0.00192	1.0
70	1490	0.00205	1.95
75	1935	0.00211	2.95
77.8	2160	0.00217	3.52
80	2370	0.00219	4.0
85	2800	0.00219	4.95
87	2930	0.00225	5.38
90			
98			
100			
108			
110	↓	↓	↓
119.8	2930	0.00225	5.38

Table 4.9: Convective Base Heating – Skirt Interior

PUMP-FED

Flight Time (Seconds)	T_{rec} (°R)	Inboard				Outboard			
		Aft Zone E1		Fwd Zone F1		Aft Zone E2		Fwd Zone E2	
		h_c	q_c	h_c	q_c	h_c	q_c	h_c	q_c
0	560	0	0	0	0	0	0	0	0
72	595								
73	600								
76.2	900								
80	1190								
85	1600								
90	2000								
90.7	2050								
96.6	2530								
99	2721	↓	↓	↓	↓	↓	↓	↓	↓
100		0	0	0	0	0	0	0	0
103		0.00376	8.2	0.00262	5.72	0.00118	2.58	0.00084	1.83
110		0.00351	7.65	0.00245	5.35	0.00111	2.42	0.00078	1.70
120		0.00318	6.92	0.00222	4.85	0.00101	2.20	0.00071	1.54
130	↓	0.00282	6.15	0.00199	4.35	0.00090	1.96	0.00063	1.38
131.5	2721	0.00279	6.08	0.00196	4.28	0.00088	1.93	000062	1.35

PRESSURE-FED

Flight Time (Seconds)	T_{rec} (°R)	Inboard				Outboard			
		Aft Zone E1		Fwd Zone F1		Aft Zone E2		Fwd Zone E2	
		h_c	q_c	h_c	q_c	h_c	q_c	h_c	q_c
0	560	0	0	0	0	0	0	0	0
59	585								
60	590								
63.9	950								
65	1060								
70	1490								
75	1935								
77.8	2160								
80	2370								
85	2800								
87	2930								
90		↓	↓	↓	↓	↓	↓	↓	↓
98		0	0	0	0	0	0	0	0
100		0.00295	7.05	0.00205	4.92	0.00093	2.22	0.00066	1.58
108									
110	↓	↓	↓	↓	↓	↓	↓	↓	↓
119.8	2930	0.00295	7.05	0.00205	4.92	0.00093	2.22	0.00066	1 .58

Table 4.10: Convective Base Heating – Skirt Exterior

approaches the heat shield. The level of heating in the inner base region between engines is approximately three times that outside the engine circle based upon model data trends. Convective heating to the interior surface of the skirt was based upon Shuttle model data trends on the OMS pod wall and body flap inboard surface. These levels of heating are shown in Table 4.9.

Convective base heating to the exterior of the skirt is listed in Table 4.10. To estimate this environment required a careful review of the plume characteristics necessary to separate the free-stream flow over the skirt. On the current STS with SRB, flow separation over the large base volume aft of the attach ring occurs at 95 seconds or 84,000 feet. Similar plume size/flow conditions on the pressure-fed LRB system would occur at 97,000 feet or approximately 98 seconds into ascent. Flow separation for the pump-fed LRB would occur about the time of thrust tail-off; approximately 103 seconds into flight. The chamber pressure decrease beyond that time would reduce the flow separation potential; but for conservatism, it was assumed to be fully applicable beyond 103 seconds. Inboard-outboard differences in the skirt exterior environment are strongly influenced by the extent of the flow separated region. The magnitudes listed in Table 4.10 reflect Shuttle flight experience.

In summary, the LRB convective base heating environment will be similar in magnitude to the Saturn V/S-1C stage environment. The pump-fed LRB will experience slightly higher levels of heating when compared with the pressure-fed concept; although turbine exhaust disposal in the nozzle moderates this difference. Convective heating will be initiated 13 seconds earlier on the pressure-fed LRB compared with the pump-fed; but the shorter burn time offsets this effect. The entire LRB base region aft of the attach ring will be immersed in hot plume gases on both concepts from approximately 100 seconds into ascent to engine shutdown.

References

[1] "Acoustic Loads Generated by the Propulsion System," NASA SP-8072, June 1971.

[2] Mullen, C. R., et. al., "Saturn Base Heating Handbook," The Boeing Co., NASA/MSFC CR-61390, May 1, 1972.

[3] Reardon, J. E., and Lee, Y. C., "Space Shuttle Main Engine Plume Radiation Model," REMTECH RTR 014-07, December 1978.

[4] Reardon, J. E., "A Computer Program for Thermal Radiation from Shuttle Exhaust Plumes (SEPRAD)," REMTECH RTR 109-01, July 1987.

[5] Goethert, B. H., "Base Flow Characteristics of Missiles with Cluster-Rocket Exhaust," Aerospace Engineering, March 1961, pps. 29, 108-117.

[6] Brewer, E. B. and Craven, C. E., "Experimental Investigation of Base Flow Field at High Altitude for a Four-Engine Cluster Nozzle Configuration," NASA TN D-5164, May 1969.

[7] Wasko, R. A. and Cover, T. L., "Experimental Investigation of Base Flow Field at High Altitudes for Configurations of Four and Five Clustered Nozzles," NASA TM X-1371, May 1967.

[8] Musial, N. T. and Ward, J. J., "Base Flow Characteristics for Several Four-Clustered Rocket Configurations at Mach Numbers from 2.0 to 3.5," NASA TN D-1073, December 1961.

[9] Charczenko, N. and Haynes, C., "Jet Effects at Supersonic Speeds on Base and Afterbody Pressures of a Missile Model Having Single and Multiple Jets," NASA TN D-2046, November 1963.

[10] Sergeant, R. J., "Base Heating Scaling Criteria for a Four-Engine Rocket Cluster Operating at High Altitude," AIAA Paper 65-286, Presented at AIAA Aerothermochemistry of Turbulent Flows Conference, December 13-15, 1965.

[11] Bender, R. L. and Reardon, J. E., "JANNAF Handbook, Rocket Exhaust Plume Technology, Chapter 5.0, Base Flow," CPIA Publication 263, July 1981.